

# On the force-free magnetosphere of aligned rotator

A. N. Timokhin\*

*Sternberg Astronomical Institute, Universitetskij pr. 13, 119992 Mocsow, Russia*

Accepted Received ; in original form

## ABSTRACT

We investigate in details properties of stationary force-free magnetosphere of aligned rotator assuming the last closed field line lying in equatorial plane at large distances from pulsar. The pulsar equations is solved numerically using multigrid code with high numerical resolution, physical properties of the magnetosphere are obtained with high accuracy. We found a set of solutions with different sizes of the closed magnetic field line zone and verify the applicability of the force-free approximation. We discuss the role of electron-positron cascades in supporting of the force-free magnetosphere and argue that the closed field line zone should grow with time slower than the light cylinder. This yield the pulsar breaking index less than 3. It is shown, that models of aligned rotator magnetosphere with widely accepted configuration of magnetic field, like one considered in this paper, have serious difficulties. We discuss solutions of this problem and argue that in any case pulsar energy losses should evolve with time differently than predicted by the magnetodipolar formula.

**Key words:** stars:magnetic fields – pulsars:general – MHD

## 1 INTRODUCTION

Since the first works on pulsar magnetosphere, a stationary force-free magnetosphere of aligned rotator is considered as an underlying model for the real pulsar magnetosphere for more than 30 years. Despite its degenerated character (such “pulsar” even does not pulse), it is believed to reproduce qualitatively all main properties of the real pulsar magnetosphere. For near-aligned pulsars it should give even an adequate detailed description. The structure of aligned rotator’s force-free magnetosphere can be described by solution of a single scalar non-linear PDE, the so-called “pulsar equation”, derived by Michel (1973b); Scharlemann & Wagoner (1973); Okamoto (1974). This is an equation for the flux of poloidal magnetic field. All other physical quantities describing the magnetosphere are related to the flux function  $\Psi$ , poloidal current  $J$  and angular velocity of magnetosphere’s rotation  $\Omega$  by algebraic relations.

Analytical solution of this equation with non-zero poloidal current seems exist only for the split-monopole configuration of the magnetic field (Michel 1991) and for a slightly perturbed split monopole (Beskin et al. 1998). For dipole magnetic field analytical solution for the case of zero poloidal current has been found (Michel 1973a; Mestel & Wang 1979), but this solution is valid only inside the light cylinder (LC). There were several works dedicated to solution of linearised pulsar equation, where poloidal current and angular velocity were assumed to be proportional

to magnetic flux function, what made the equation linear, but they did not lead to construction of a consistent model of aligned rotator magnetosphere (see e.g. Beskin et al. 1983; Lyubarskii 1990; Beskin & Malyshekin 1998).

The first attempt to solve this equation numerically was made by Contopoulos et al. (1999), hereafter CKF. They have shown for the first time, that there exists a *self-consistent* solution with dipole magnetic field geometry near the NS and magnetic field lines smoothly passing through the light cylinder. In that work the position of the null point<sup>1</sup> was fixed at the light cylinder and the question about applicability of the force-free approximation have been not investigated. Energy losses of the aligned rotator for CKF solution have been calculated by Gruzinov (2005). Goodwin et al. (2004) have studied this problem more deeply, namely they have searched for solution of the pulsar equation when the position of the null point is not fixed at the LC, but lies at different positions inside the light cylinder. For any position of the null point they obtained solutions, smoothly passing the light cylinder, but like CKF they have not studied physical properties of obtained solutions (e.g. energy losses, applicability of the force-free approximations etc.). Their model, however, seems to be artificial, because they assumed non-zero pressure in the closed field line zone, what implies continuous energy injection into the closed field line domain. Recently Contopoulos (2005)

<sup>1</sup> the point where the last closed field line intersects the equatorial plane

\* E-mail: atim@sai.msu.ru

addressed the case when the plasma rotation frequency in the open field line domain is different from the rotation frequency of the NS. It was shown, that there exist an unique solution of the pulsar equation for arbitrary plasma rotation frequency, although a rather simple case when the plasma rotation frequency is constant have been considered. Applicability of the force-free approximations in the magnetosphere of aligned rotator was considered in Timokhin (2005) and Contopoulos (2005), though in the latter work only for the null point located at the LC.

Recently a different approach to the pulsar magnetosphere modelling is being developed by Spitkovsky (2005), Komissarov (2005), and McKinney (2006). They perform *time-dependent* simulations of the pulsar magnetosphere. In Komissarov (2005) aligned rotator magnetosphere was modelled using full MHD code, in McKinney (2006) the same modelling was done with force-free code. The code of Anatoly Spitkovsky allows performing of 3-D time-dependent simulation of the magnetosphere of inclined rotator by solving equations of force-free MHD. In these simulations the *existence* of the stationary force-free magnetospheric configuration was rigorously proved for the first time. Although this approach presents a big step towards the modelling of the real pulsar magnetosphere, in this paper we argue that it has serious limitation, namely the properties of cascades supplying particles in magnetosphere are not incorporated in these simulations. As it will be discussed later, cascades can set non-trivial boundary conditions on the current density in the magnetosphere. Its incorporation in time-dependent codes would require some efforts.

In this work we investigate stationary problem solving the pulsar equation numerically with high numerical resolution. We assume zero pressure in the closed field line region (cold plasma). As in all above mentioned works on numerical modelling of stationary aligned rotator magnetosphere we assume a topology with the current sheet in open field line domain flowing in the equatorial plane, i.e. configuration with Y null point – see Fig. 1. This type of magnetosphere topology had became de facto the “standard model”, so we study it in details and analyse its properties regarding many aspects of electrodynamics. Smooth solutions are obtained for *any* position of the null point inside the light cylinder. High numerical resolution allows accurately incorporation of the return current flowing along the separatrix into numerical procedure. With the high resolution of used numerical method it was possible to calculate accurately physical properties of the solutions such as Goldreich-Julian charge density, magnetic field, energy losses and pointing flux distribution etc., check applicability of the force-free approximation and consider compatibility of the model with models of electron-positron cascades.

Adjustment of the current density in the polar cap cascade zone of pulsar to the global magnetospheric structure was debated already in the first ten years after pulsar discovery (see e.g. Arons 1979). A concrete mechanism for the current density adjustment was proposed by Yu. Lyubarskij many years later, in 1992. At that time there was no self-consistent model of pulsar magnetosphere and detailed discussion on this subject was difficult. Here we discuss the coupling between the polar cap cascade zone and the rest of the magnetosphere in the frame of the self-consistent model obtained in our simulations. We extend the picture proposed

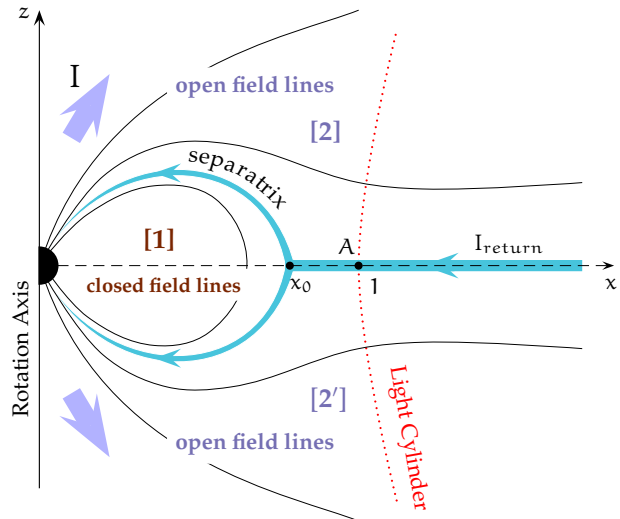


**Figure 1.** Configuration of magnetic field in the magnetosphere of aligned rotator with Y null point – Y-configuration. After the null point  $x_0$  the separatrix goes along the equatorial plane. The volume current  $I$  flowing in the open field line zones [2] and [2'] closes somewhere beyond the light cylinder. There could be a volume return current along some open field lines, but the largest part of it flows along the separatrix.

by Lyubarskij (1992) addressing the evolution of the current adjustment mechanism with ageing of the pulsar. We also prove the necessity of such mechanism and discuss it in more details in the frame of the cascade model proposed by Scharlemann et al. (1978). We underline serious difficulties of model with Y null point regarding its compatibility with the Space Charge Limited Flow models of polar cap cascades and briefly discuss other possible magnetospheric configuration.

The plan of the paper is the following. In Section 2 important properties of the pulsar equation are discussed. Model used in the current work and numerical method are described in Section 3. Results of numerical simulations are presented in Section 4. In section 5 we discuss the role of polar cap cascades for the global structure of the magnetosphere, consider in details properties of the force-free magnetosphere with Y null point, and highlight problems of the “standard” model of aligned rotator magnetosphere. A different topology of the magnetosphere, with X null point, is briefly discussed at the end of the section. We summarise the most important results in Section 6.

## 2 THE PULSAR EQUATION

### 2.1 General equation

Here we adopt the wide used assumption, that the *entire* magnetosphere of the neutron star (NS) is filled with plasma. In some works starved magnetosphere configuration have been debated (see e.g. Smith et al. 2001; Pétri et al. 2002), where there are several separated clouds of charged particles near the NS and no particle outflow, however there are indications that such configuration is unstable against diocotron instability (Spitkovsky & Arons 2002; Spitkovsky 2004). Plasma in the magnetosphere has to be non-neutral

in order to screen the longitudinal (directed along magnetic field lines) component of the electric field, induced by rotation of the NS. In presence of the longitudinal electric field charged particles would be accelerated and their radiation will lead to copious electron-positron pair production in super-strong magnetic field of pulsar (Sturrock 1971), what finally results in screening of the accelerating field.

Charge density necessary for cancelling of the longitudinal electric field, the so-called Goldreich-Julian (GJ) charge density (Goldreich & Julian 1969), near the neutron star is given by

$$\rho_{\text{GJ}} \simeq -\frac{\boldsymbol{\Omega} \cdot \mathbf{B}}{2\pi c}, \quad (1)$$

where  $\boldsymbol{\Omega}$  is angular velocity on neutron star rotation,  $\mathbf{B}$  is magnetic field and  $c$  is the speed of light. Assuming that NS has dipolar magnetic field, the ratio of the particle kinetic energy density in the magnetosphere to the energy density of the magnetic field at the distance  $r$  can be estimated as

$$\begin{aligned} \frac{\varepsilon_{\text{kin}}}{\varepsilon_B} &\sim \frac{(\rho_{\text{GJ}}/e) m_e c^2 \gamma}{(B^2/8\pi)} \simeq \\ &\simeq 1.4 \times 10^{-11} P^{-1} \left(\frac{\gamma}{10^7}\right) \left(\frac{B_0}{10^{12} \text{G}}\right)^{-1} \left(\frac{r}{R_{\text{NS}}}\right)^3, \end{aligned} \quad (2)$$

where  $e$  and  $m_e$  are electron charge and mass correspondingly,  $R_{\text{NS}}$  – neutron star radius,  $\gamma$  – Lorentz factor of accelerated particles,  $B_0$  magnetic field strength in Gauss near magnetic poles of the star and  $P$  – period of pulsar rotation in seconds. All these quantities are normalised to their typical values in pulsars. This ratio is small, less than 1 per cent, in the region with the size  $\sim 10^3 P^{-1}$  radii of the neutron star. It could remain small even further, but here magnetic field deviates substantially from the NS's dipole field due to currents flowing in the magnetosphere, and  $\varepsilon_{\text{kin}}/\varepsilon_B$  can be estimated only after a self-consistent solution for the magnetosphere structure is found. So, in a large domain surrounding the neutron star, we can use force-free approximation, when particle inertia is neglected, and equation of motion takes the form

$$\rho \mathbf{E} + \frac{1}{c} [\mathbf{j} \times \mathbf{B}] = 0. \quad (3)$$

Hence, electric field  $\mathbf{E}$  is perpendicular to the magnetic field  $\mathbf{B}$ . Charge density  $\rho$  and current density  $\mathbf{j}$  in eq. (3) can be found from the Maxwell equations (we consider stationary problem)

$$\nabla \cdot \mathbf{E} = 4\pi \rho, \quad (4)$$

$$\nabla \times \mathbf{B} = \frac{4\pi}{c} \mathbf{j}, \quad (5)$$

With help of these equations equation (3) can be written as

$$(\nabla \cdot \mathbf{E}) \mathbf{E} + [\nabla \times \mathbf{B}] \times \mathbf{B} = 0. \quad (6)$$

In the force-free electrodynamics (FFE)<sup>2</sup> the only possible motion of charged particles across magnetic field lines is the drift in crossed electrical and magnetic fields with the velocity

$$\mathbf{U}_{\text{D}} = c \frac{\mathbf{E} \times \mathbf{B}}{B^2}. \quad (7)$$

<sup>2</sup> hereafter we use this shorter name for force-free degenerate electrodynamics (see e.g. Komissarov 2002; Blandford 2002, and references there)

Obviously  $|\mathbf{U}_{\text{D}}|$  must be less than  $c$ , or equivalently  $E$  must be less than  $B$ . Generally speaking, eq. (3) can have solutions where  $|\mathbf{U}_{\text{D}}| > c$ . The surface, where  $|\mathbf{U}_{\text{D}}|$  reaches  $c$ , is commonly referred as the *light surface*. Beyond the light surface, where  $|\mathbf{U}_{\text{D}}| > c$ , the force-free approximation can not be applied. FFE is not self-consistent, because particle dynamics is ignored. Hence, each solution of eq. (6) should be always checked for applicability of the force free approximation.

In the axisymmetric stationary case considered here magnetic field in cylindrical coordinates  $(\varpi, \phi, Z)$  can be written as

$$\mathbf{B} = \frac{\nabla \Psi \times \mathbf{e}_\phi}{\varpi} + \frac{4\pi I}{c \varpi} \mathbf{e}_\phi, \quad (8)$$

where  $\mathbf{e}_\phi$  is the unit azimuthal, toroidal vector. In components

$$(B_\varpi, B_\phi, B_Z) = \left(-\frac{1}{\varpi} \partial_Z \Psi, \frac{4\pi I}{c \varpi}, \frac{1}{\varpi} \partial_\varpi \Psi\right). \quad (9)$$

Scalar function  $\Psi$  is related to the magnetic flux  $\Phi_{\text{mag}}$  through the circle with the centre at the point  $(0, Z)$  and radius  $\varpi$  by  $\Phi_{\text{mag}} = 2\pi \Psi(\varpi, Z)$ . So, lines of constant  $\Psi$  coincides with magnetic field lines. It could be easily verified, that in force-free case the scalar function  $I(\varpi, Z)$  is constant along magnetic field lines, i.e

$$I \equiv I(\Psi). \quad (10)$$

$I$  is related to the total current  $J$  outflowing through the above mentioned circle by  $J = 2\pi I(\varpi, Z)$ .

In the quasi-stationary case the time derivative of  $\mathbf{B}$  takes the form (see Mestel 1973)

$$\frac{\partial \mathbf{B}}{\partial t} = \nabla \times ([\boldsymbol{\Omega} \times \mathbf{r}] \times \mathbf{B}). \quad (11)$$

Substituting this into the Faraday's law

$$\nabla \times \mathbf{E} = -\frac{1}{c} \partial_t \mathbf{B}, \quad (12)$$

we get for the electric field

$$\mathbf{E} = -\frac{\boldsymbol{\Omega} \times \mathbf{r}}{c} \times \mathbf{B} - \nabla V = -\frac{\Omega}{c} \nabla \Psi - \nabla V, \quad (13)$$

where  $V$  is the non-corotational (see below) part of electric potential. The first term in (13) is poloidal and only the second term could make a contribution to the toroidal component. In axisymmetric case  $\partial_\phi V = 0$  and, hence,  $\mathbf{E}$  is poloidal. In the force-free case  $\mathbf{E} \perp \mathbf{B}$ , from this follows that  $\mathbf{E} \cdot (\nabla \Psi \times \mathbf{e}_\phi) = 0$ . Consequently,  $\mathbf{E} \propto \nabla \Psi$  and we can write

$$\mathbf{E} = -\frac{\Omega_{\text{F}}}{c} \nabla \Psi, \quad (14)$$

or in components

$$(E_\varpi, E_\phi, E_Z) = \left(-\frac{\Omega_{\text{F}}}{c} \partial_\varpi \Psi, 0, -\frac{\Omega_{\text{F}}}{c} \partial_Z \Psi\right). \quad (15)$$

Substituting this expression together with eq. (8) into the formula for the drift velocity (7), we get

$$\mathbf{U}_{\text{D}} = \Omega_{\text{F}} \varpi \mathbf{e}_\phi - \frac{4\pi I \Omega_{\text{F}}}{c B^2} \mathbf{B} \equiv \boldsymbol{\Omega}_{\text{F}} \times \mathbf{r} - \kappa \mathbf{B}. \quad (16)$$

So, the particle motions is composed from rotation with the angular velocity  $\Omega_{\text{F}}$  and gliding along magnetic field lines.

Hence,  $\Omega_F$  is the angular velocity of magnetic field lines rotation. By substitution of eq.(14) into the stationary Faraday's law one find  $\nabla\Omega_F \times \nabla\Psi = 0$ . This implies that  $\Omega_F$  is constant along magnetic field lines:

$$\Omega_F \equiv \Omega_F(\Psi). \quad (17)$$

Equation (17) is the well known Ferraro isorotation law.

Finally, substituting  $\mathbf{E}$  and  $\mathbf{B}$  from eqs. (8), (14) into equation (6) we get

$$\left(1 - \frac{\Omega_F^2 \varpi^2}{c^2}\right) \nabla^2 \Psi - \frac{2}{\varpi} \partial_{\varpi} \Psi + \left(\frac{4\pi}{c}\right)^2 I \frac{dI}{d\Psi} - \frac{\varpi^2}{c^2} \Omega_F \frac{d\Omega_F}{d\Psi} (\nabla\Psi)^2 = 0 \quad (18)$$

This is Grad-Shafranov equation for the poloidal magnetic field, the so-called pulsar equation, derived by Michel (1973b); Scharlemann & Wagoner (1973); Okamoto (1974). This scalar PDE is of elliptical type. It is the poloidal part of the vector equation (6). The toroidal part of eq. (6) is simply the relation (10). Pulsar equation has two integrals of motion –  $I$  and  $\Omega_F$ . If we know them, we can solve this equation for function  $\Psi$  and determine the poloidal magnetic field. Electric and magnetic fields and all other parameters of the force-free magnetosphere can be found, because they are connected to  $\Psi$ ,  $I$  and  $\Omega_F$  by algebraic relations. In the frame of FFE  $I$  and  $\Omega_F$  are *free parameters*. They could be determined self-consistently in the full MHD, if also electromagnetic cascades, setting boundary conditions, are taken into account (see Beskin 2005). Nevertheless one can get useful results in the force-free approximation. Equation (18) has one singular surface, the so-called *light cylinder* (LC), where  $\varpi = c/\Omega_F(\Psi(\varpi, Z))$ . As it will be shown in the next subsection the difference between  $\Omega_F$  and  $\Omega$  is small and the singular surface has shape close to a cylinder with the radius of  $R_{LC} = c/\Omega$ .

We normalise variables  $\varpi$  and  $Z$  to  $R_{LC}$  and introduce new dimensionless coordinates  $x \equiv \varpi/R_{LC}$  and  $z \equiv Z/R_{LC}$ . We will consider the case of dipolar magnetic field on the NS. So, near the star the magnetic field is given by

$$\Psi = \mu \frac{\varpi^2}{(\varpi^2 + Z^2)^{3/2}} \equiv \Psi_0 \frac{x^2}{(x^2 + z^2)^{3/2}}, \quad (19)$$

where  $\mu = B_0 R_{NS}^3/2$  is the magnetic moment of the NS and  $\Psi_0 \equiv \mu/R_{LC}$ . We normalise  $\Psi$  to  $\Psi_0$  and introduce dimensionless function  $\psi \equiv \Psi/\Psi_0$ . Instead of poloidal current function  $I$  we introduce dimensionless function  $S \equiv (4\pi/c)(R_{LC}/\Psi_0)I$ . Angular velocity of magnetic field line rotation is normalised to the angular velocity of the NS by the relation  $\Omega_F(x, z) \equiv \beta(x, z)\Omega$ . For these dimensionless functions the pulsar equation (18) takes the form

$$(\beta^2 x^2 - 1)(\partial_{xx}\psi + \partial_{zz}\psi) + \frac{\beta^2 x^2 + 1}{x} \partial_x \psi - S \frac{dS}{d\psi} + x^2 \beta \frac{d\beta}{d\psi} (\nabla\psi)^2 = 0. \quad (20)$$

At the light cylinder the coefficient by second derivatives goes to zero and the pulsar equation has the form

$$2\beta \partial_x \psi = S \frac{dS}{d\psi} - \frac{1}{\beta} \frac{d\beta}{d\psi} (\nabla\psi)^2. \quad (21)$$

Let us now discuss properties of functions  $\Omega_F$  and  $S$ .

## 2.2 $\Omega_F$

From relations (17) it follows that  $V$  is constant along a magnetic field line. Hence, we could rewrite eq. (13) in the following form

$$\mathbf{E} = -\frac{1}{c} \left( \Omega + c \frac{\partial V}{\partial \Psi} \right) \nabla \Psi. \quad (22)$$

Comparing this expression with eq. (14) we get

$$\Omega_F = \Omega + c \frac{\partial V}{\partial \Psi}. \quad (23)$$

If there were no potential difference between different magnetic field lines and between them and the surface of the pulsar,  $\Omega_F$  were equal to  $\Omega$ . But, independently of NS surface properties, a potential difference along open magnetic field lines will be always build in polar cap region of pulsar (Ruderman & Sutherland 1975; Scharlemann et al. 1978; Muslimov & Tsygan 1992). This lead to formation of a particle acceleration zone, where force-free approximation is not valid and charged particles are accelerated by the longitudinal electric field. Electron-positron pairs produced in the strong magnetic field of pulsar by photons, emitted by accelerated particles, screen the accelerating field, and as pair-production rate grows very rapidly with the distance, acceleration zone terminates in a rather thin layer called pair-formation front (PFF). Above PFF accelerating field is screened and FFE can be applied. The size of the acceleration zone is small compared to the overall size of the magnetosphere, its height varies from  $\sim 100$  m for young pulsars in model with no particle escape from the NS surface (Ruderman & Sutherland 1975) to 1-2 stellar radii in models, where particles freely escape the star surface (Scharlemann et al. 1978; Muslimov & Tsygan 1992). Geometrically this small region could be neglected in the modelling of the global magnetospheric structure. The potential difference between NS surface and magnetic field lines should be taken into account by boundary conditions on  $V$ , which can be reformulated as boundary conditions on  $\Omega_F$ . Potential difference along a magnetic field line in the acceleration zone is determined by the position of PFF, which depends on local geometry of magnetic field, close to the NS surface, and kinetic processes in the electron-positron cascade.

By the order of magnitude the relative difference of rotation velocities of plasma and NS can be estimated as

$$\frac{\delta\Omega}{\Omega} \equiv \frac{\Omega - \Omega_F}{\Omega} \simeq \frac{P}{2\pi r_{pc}} \frac{v_{rot}}{c} \simeq 2.28 \times 10^{-11} \left( \frac{B_0}{10^{12} \text{ G}} \right)^{-1} P^2 \Delta V, \quad (24)$$

where  $\Delta V$  is potential difference between NS surface and PFF (in esu units),  $r_{pc} \simeq \sqrt{R_{NS}^3 \Omega/c}$  is the size of the polar cap;  $v_{rot} = c\Delta V/(B_0 r_{pc})$  is the linear velocity of plasma rotation relative to the NS surface in the acceleration zone – see eq. (31) in Ruderman & Sutherland (1975).

In the model with no particle escape from the NS surface the potential difference is given by (Ruderman & Sutherland 1975, equation (23))

$$\Delta V \simeq 5.24 \times 10^9 P^{-1/7} \left( \frac{\rho_c}{10^6 \text{ cm}} \right)^{4/7} \left( \frac{B_0}{10^{12} \text{ G}} \right)^{-1/7}, \quad (25)$$

where  $\rho_c$  is the curvature radius of magnetic field lines. The potential difference is measured in esu units. Substituting these expression into eq. (24) we get

$$\frac{\delta\Omega}{\Omega} \simeq 0.1 P^{13/7} \left( \frac{\rho_c}{10^6 \text{cm}} \right)^{4/7} \left( \frac{B_0}{10^{12} \text{G}} \right)^{-8/7}. \quad (26)$$

We see, that for relatively young pulsars, with periods  $P \lesssim 0.3$  s, this ratio is very small,  $\sim 1$  per cent. Even if the field line curvature radius is of the order of  $\sim 10^8$  cm, typical for dipole magnetic field, for  $P \lesssim 0.1$  s this ratio is  $\sim 2$  per cents.

For the model where particles freely escape the NS surface we use estimations from Hibschan & Arons (2001). The potential difference in the acceleration zone (Hibschan & Arons 2001, eqs. (17) and (18))

$$\Delta V^{h > r_{\text{pc}}} \simeq 9.87 \times 10^9 P^{-2} \left( \frac{B_0}{10^{12} \text{G}} \right) h, \quad (27)$$

$$\Delta V^{h < r_{\text{pc}}} \simeq 1.11 \times 10^{12} P^{-3/2} \left( \frac{B_0}{10^{12} \text{G}} \right) h^2. \quad (28)$$

Here  $h$  is the height of PFF above the NS surface in units of  $R_{\text{NS}}$ . The above estimations for accelerating potential are for the cases when when  $h > r_{\text{pc}}$  and  $h < r_{\text{pc}}$  correspondingly. The potential differences are in esu units. The heights of PFF position due to photons emitted by non-resonant inverse Compton scattering (NIC), curvature radiation (CR) and resonant inverse Compton scattering (RIC) of accelerated particles are given by

$$h_{\text{NIC}} \simeq 0.40 P \left( \frac{B_0}{10^{12} \text{G}} \right)^{-1} T_6^{-2} f_\rho \quad (29)$$

$$h_{\text{NIC}}^c \simeq 0.12 P^{1/4} \left( \frac{B_0}{10^{12} \text{G}} \right)^{-1/2} T_6^{-1} f_\rho^{1/2} \quad (30)$$

$$h_{\text{CR}} \simeq 0.68 P^{19/12} \left( \frac{B_0}{10^{12} \text{G}} \right)^{-5/6} f_\rho^{1/2} \quad (31)$$

$$h_{\text{RIC}} \simeq 12 \left( \frac{B_0}{10^{12} \text{G}} \right)^{-7/3} T_6^{-2/3} f_\rho, \quad (32)$$

see Hibschan & Arons (2001), eqs. (34), (32), (42) and (37) correspondingly. Label ‘‘c’’ correspond to the model where the NS surface is colder than the polar cap of the pulsar, heated by the return current.  $T_6$  is the temperature of the polar cap in units of  $10^6$  K. The radius of curvature of magnetic field lines is factor  $f_\rho$  times the radius of curvature of a dipole field, i.e.  $f_\rho \equiv \rho_c / \rho_c^{\text{dip}} = P^{-1/2} \rho_c / (9.2 \times 10^7 \text{cm})$ .

According to Hibschan & Arons (2001), in most pulsar the PFF height is set by non-resonant ICS photons. In high voltage pulsar, ones with the shortest periods – millisecond and youngest pulsar with  $P \lesssim 0.3$  s, the PFF is set by curvature photons. In both of these cases the resulting height of the PFF is larger, than the size of the polar cap,  $h > r_{\text{pc}}$ . Resonant ICS is important only for high field pulsars, with  $B \gtrsim 1.2 \times 10^{13}$  G, in this case  $h \ll r_{\text{pc}}$ . Taking this into account we get

$$\left( \frac{\delta\Omega}{\Omega} \right)_{\text{NIC}} \simeq 0.09 P f_\rho T_6^{-2} \left( \frac{B_0}{10^{12} \text{G}} \right)^{-1} \quad (33)$$

$$\left( \frac{\delta\Omega}{\Omega} \right)_{\text{NIC}}^c \simeq 0.027 P^{1/4} f_\rho^{1/2} T_6^{-1} \left( \frac{B_0}{10^{12} \text{G}} \right)^{-1/2} \quad (34)$$

$$\left( \frac{\delta\Omega}{\Omega} \right)_{\text{CR}} \simeq 0.023 \left( \frac{P}{0.3 \text{s}} \right)^{19/12} f_\rho^{1/2} \left( \frac{B_0}{10^{12} \text{G}} \right)^{-5/6} \quad (35)$$

$$\left( \frac{\delta\Omega}{\Omega} \right)_{\text{RIC}} \simeq 0.034 P^{1/2} f_\rho^2 T_6^{-4/3} \left( \frac{B_0}{1.2 \times 10^{13} \text{G}} \right)^{-14/3} \quad (36)$$

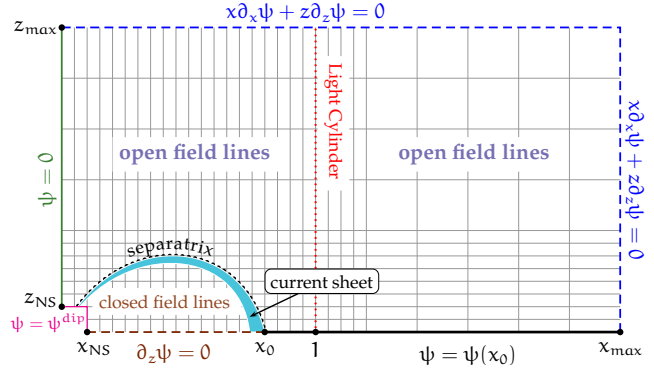


**Figure 2.** Calculation domain and imposed boundary conditions. See text for explanation.

The temperature of the polar cap  $T$  due to the heating by return particles is of the order of  $10^6$  K. If the NS temperature is higher than this value, than formula (33) should be applied, in the opposite case – formula (34). The temperature of the NS surface depend of neutron star cooling model, and for rather young pulsar it should be higher than  $10^6$  K. So, formula (33) is applicable for young, hot pulsar, where it gives for  $\delta\Omega/\Omega \simeq 0.01$ . Hence, in the model with free particle escape, the ratio  $\delta\Omega/\Omega$  is of the order of few per cents for the majority of pulsars.

We see, that  $1 - \beta$  is of order of few per cents for most pulsars in the model with free particle escape and for young pulsars in the model with no particles escape. We restrict ourself considering only such pulsars, where  $1 - \beta$  is small. Then the last term in pulsar equation (38) is small in comparison with other terms and could be neglected. In the rest of the paper we assume

$$\Omega_F \equiv \Omega. \quad (37)$$

This assumption simplifies the pulsar equation (20), which now has the form

$$(x^2 - 1)(\partial_{xx}\psi + \partial_{zz}\psi) + \frac{x^2 + 1}{x}\partial_x\psi - SS' = 0, \quad (38)$$

where  $S' \equiv dS/d\psi$ . Nonlinearity in this equation is now present only in the term with the poloidal current function  $S$ .

### 2.3 Poloidal current $S$

In contrast to  $\Omega_F$ , being set by kinetic processes in the polar cap,  $S$  depends on the global structure of the magnetosphere. Both inside and outside the light cylinder the pulsar equation (38) is a regular non-linear PDE of elliptic type. At the light cylinder this equation under assumption (37) has the form

$$\partial_x\psi = \frac{1}{2}SS'. \quad (39)$$

If function  $S$  is known, condition (39) can be considered as a Neumann type boundary condition at the light cylinder. If boundary conditions are set both inside and outside the LC, the equation should have an unique solution in both regions. Generally speaking, for arbitrary function  $S$  solutions of the pulsar equation inside and outside the LC will not match,

$$\lim_{x \rightarrow 1^-} \psi \neq \lim_{x \rightarrow 1^+} \psi. \quad (40)$$

So, a smooth<sup>3</sup> solution is possible only for a specific function  $S$  and the problem of finding a solution of the pulsar equations becomes an eigenvalue problem for the function  $S$ .

The position of the light cylinder is not known a priori. For  $\Omega_F$  different from  $\Omega$  it has a rather complicated form and, even if  $\Omega_F(\Psi)$  as a function of  $\Psi$  is given by a model of the polar cap cascade, the position of the LC as a function of  $x$  and  $z$  has to be found self-consistently together with the solution of the pulsar equation. However, as it was stressed above, for most pulsars the deviation of the LC from a cylinder with the radius  $c/\Omega$  is of the order of few per cents or less. Hence, a solution of equation (38) should give a very good approximation to the real magnetosphere of aligned rotator.

The other open question regarding the poloidal current term in the pulsar equation is the topology of the magnetosphere. In works of the Lebedev Physical Institute group (see e.g. Beskin et al. 1993; Beskin & Mal'yskin 1998) a geometry with X null point have been assumed, hereafter X-configuration, see Fig. 13(a). In that case the pulsar equation should be solved in 3 different domains, separated by the current sheets. The positions of the point  $A$  (and  $A'$ ) is a free parameter of such model. Setting the positions of these points and the point  $x_0$  one fixes the boundaries and gets a well posed, although complicated, problem. Such topology of the aligned rotator magnetosphere was criticised by Lyubarskii (1990), because the only source of the magnetic field in the magnetosphere is the pulsar itself, and in this case it is not clear what would be the source of the magnetic field in the outer domain. The most frequently considered topology of the aligned rotator magnetosphere implies an Y-like null point, hereafter Y-configuration, see Fig. 1. In this case the only available free parameter in the model is the position of the null point  $x_0$ . Fixing position of this point we fix the whole geometry of the magnetosphere. So, we have an elliptic equation with boundary conditions set at all boundaries of the closed domains with known positions of the boundaries. We wish to emphasise here, that the choice of the magnetosphere's topology is an additional assumption in the frame of stationary problem. In the following we investigate in details the force-free magnetosphere of aligned rotator assuming topology with an Y-like neutral point.

### 3 NUMERICAL MODEL

We solve equation (38) in a rectangular domain, see Fig. 2. The boundary conditions are the following. On the rotation axis ( $z$ -axis)

$$\psi(0, z) = 0, \quad z_{\text{NS}} < z \leq z_{\text{max}}. \quad (41)$$

At the equatorial plane, in the closed field line zone

$$\partial_z \psi(x, 0) = 0, \quad x_{\text{NS}} < x < x_0, \quad (42)$$

following from the symmetry of the system. In the open field line domain

$$\psi(x, 0) = \psi(x_0, 0), \quad x_0 < x \leq x_{\text{max}}, \quad (43)$$

i.e. the separatrix lies in the equatorial plane. Close to the NS the magnetic field is assumed to be dipolar, so for  $x = x_{\text{NS}}, 0 \leq z \leq z_{\text{NS}}$  and  $0 \leq x \leq x_{\text{NS}}, z = z_{\text{NS}}$

$$\psi(x, z) = \psi^{\text{dip}}(x, z) \equiv \frac{x^2}{(x^2 + z^2)^{3/2}}. \quad (44)$$

Magnetic surfaces should become radial at large distance from the NS, see Ingraham (1973). On the other hand, in calculations of Contopoulos et al. (1999), where pulsar equation was solved in the unbounded domain, with boundary conditions at infinity implying finiteness of the total magnetic flux, magnetic surfaces became nearly radial already at several sizes of the light cylinder. Rather different outer boundary conditions, with finite magnetic flux inside the light cylinder at infinity, have been used by Sulkanen & Lovelace (1990). However, time-dependent simulations of Komissarov (2005); Spitkovsky (2005) and McKinney (2006) provide strong evidence for correctness of outer boundary conditions when magnetic surfaces at large distances from the NS are radial. So, at the outer boundaries of the calculation domain for  $0 < x \leq x_{\text{max}}, z = z_{\text{max}}$  and  $x = x_{\text{max}}, 0 < z \leq z_{\text{max}}$

$$x \partial_x \psi + z \partial_z \psi = 0. \quad (45)$$

At the light cylinder two conditions should be satisfied:

(i) the solution should be continuous,

$$\psi(x \rightarrow 1^-, z) = \psi(x \rightarrow 1^+, z), \quad (46)$$

and (ii) the condition (39). These conditions together provide smooth transition through the LC. Following Goodwin et al. (2004) we expand function  $\psi$  at the LC in Taylor series over  $x$  implying continuity condition (46). By substituting the resulting expansion into the pulsar equation (38) and retaining the terms up to the second order we get the following approximation to the pulsar equation at the LC

$$4 \partial_{xx} \psi(1, z) + 2 \partial_{zz} \psi(1, z) = \partial_x [SS'(1, z)]. \quad (47)$$

This equation is nothing more than a reformulation of the smoothness conditions (46), (39) valid for the first and second order terms in Taylor series expansion of  $\psi$ . As the numerical scheme we have used is of the second order, this approximation, as well as its discretization, has the same accuracy as the discretized equation in the rest of the numerical domain. In course of relaxation procedure we are trying to satisfy the conditions (46), (39), i.e. we solve equation (47) at the LC instead of the original equation (38), which is singular there. Equation (39) is used for determination of the poloidal current term  $SS'(\psi)$  along the open field lines.

In the closed field lines zone,  $\psi > \psi_{\text{last}} \equiv \psi(x_0, 0)$ , there is no poloidal current, so  $SS' \equiv 0$ . The return current needed to keep the system charge neutral flows along the separatrix. In the open field line domain by setting the boundary condition (43) the presence of an infinite thin current sheet is already incorporated into the solution procedure. However, when the separatrix goes above the equatorial plane we have to model the current sheet. We assume that the return current is flowing along the field lines corresponding to the magnetic surfaces  $[\psi_{\text{last}}, \psi_{\text{last}} + d\psi]$ . The total return

<sup>3</sup> if solution is continuous its smoothness follows from eq. (39), because  $SS'$  is the same at both sides of the LC.

current flowing in this region is calculated by integration of the term  $SS'$ :

$$S_{\text{return}} = \sqrt{2 \int_0^{\psi_{\text{last}}} SS' d\psi}. \quad (48)$$

We model the poloidal current density distribution over  $\psi$  in the current sheet  $\psi_{\text{last}} \leq \psi \leq \psi_{\text{last}} + d\psi$  by an even order polynomial function going to zero at the boundaries of the current sheet

$$S'(\psi) = A \left[ \left( \psi - \left( \psi_{\text{last}} + \frac{d\psi}{2} \right) \right)^{2k} - \left( \frac{d\psi}{2} \right)^{2k} \right], \quad (49)$$

where constant  $A$  is determined from the requirement  $\int_0^{\psi_{\text{last}}+d\psi} S(\psi) d\psi = 0$  and  $k$  is an integer constant. The pulsar equation is then solved in the whole domain including the current sheet. Although the current sheet cannot be considered as a force-free domain, but doing so we calculate correct the influence of the current sheet on to the global magnetospheric structure, though the obtained values of the physical parameters *inside* the current sheet are fake.

We developed a multigrid numerical scheme for solution of equations (38) and (47). These equations have been discretized using the 5-point Gauss-Seidel rule. The coarsest numerical grid was constructed in the way, that the light cylinder is at cell boundaries. Each subgrid was obtained by halving of the previous grid. Cell sizes in the region  $x < 1, z < 1$  are smaller in order to accurately calculate the current along the separatrix. We used FAS scheme with V-type cycles (see Trottenberg et al. 2001). The Gauss-Seidel scheme was used as both smoother and solver at the coarsest level. At each iteration step both in the solver and smoother the new value of the poloidal current term  $SS'(1, z)$  was calculated from the relation (39) at each point of the LC. Then a piece-polynomial interpolation of  $SS'$  in the interval  $(0, \psi_{\text{last}})$  was constructed and the return current distribution was calculated according to the formulae (48) and (49). Then for each point  $(x, z)$  in the calculation domain the current term was calculated as  $SS'(x, z) = SS'(\psi(x, z))$ , and the new iteration was started. So, we solved the pulsar equation in the whole domain avoiding a very time consuming matching of the solutions inside and outside the light cylinder as it was done by Contopoulos et al. (1999); Contopoulos (2005) and Gruzinov (2005), though in Contopoulos (2005) this matching procedure have been accelerated. As a starting configuration a dipolar magnetic field everywhere was used. We did not encounter any problems with the convergence of the scheme for any value of  $x_0$ , but for  $x_0$  very close to 1 the convergence rate becomes essentially slower. Typical number of points along each directions we used in the calculations was 3000 – 6000.

We performed calculations for different values of numerical parameters in order to proof the independence of the results on the domain sizes  $(x_{\text{max}}, z_{\text{max}})$ , the “NS size”  $(x_{\text{NS}}, z_{\text{NS}})$ , the width of the current sheet  $d\psi$  and the form of the current distribution (parameter  $k$ ), as well as on the iteration procedure stopping criteria and number of points along both directions. Changes in convergence criteria and decreasing of the cell size from ones used in the most of our calculations did not produce relative changes in solutions greater than  $10^{-4}$ . In Table 1 values of  $\psi_{\text{last}}$  and energy

**Table 1.** Properties of obtained solution with  $x_0=0.7$  and  $x_0$  approaching the LC for different values of numerical parameters

$d\psi$	numerical parameters:			results:	
	$2k$	$(x_{\text{max}}, z_{\text{max}})$	$(x_{\text{NS}}, z_{\text{NS}})$	$\psi_{\text{last}}$	$W$
$x_0=0.7$					
0.03	2	(8,7)	(0.0667, 0.056)	1.717	1.864
0.03	4	(8,7)	(0.0667, 0.056)	1.712	1.853
0.015	2	(8,7)	(0.0667, 0.056)	1.697	1.821
0.03	2	(8,7)	(0.0333, 0.028)	1.720	1.870
0.03	2	(16,14)	(0.0667, 0.056)	1.717	1.864
$x_0=0.99$					
0.08	2	(16,14)	(0.06, 0.06)	1.255	0.977
$x_0=0.99231$					
0.04	2	(5,5)	(0.0462, 0.0525)	1.230	0.939

losses of aligned rotator  $W$  (see next section), obtained in computations with different values of listed numerical parameters, are shown for  $x_0 = 0.7$  and  $x_0$  approaching the light cylinder. One can see, that with an accuracy of the order of few per cents obtained solutions are independent on particular values of the numerical parameters. Solutions with other  $x_0$ 's have similar behaviour.

## 4 RESULTS OF CALCULATIONS

Our choice of the boundary conditions at the NS, equation (44), corresponds to the case when the dipole magnetic moment of the star  $\mu$  is parallel to the angular velocity vector  $\Omega$ ,  $\mu \parallel \Omega$ . In this case the GJ charge density in the polar cap of pulsar is negative and there are electrons, which flow away from the polar cap. The poloidal current  $S$  in the open field line zone is negative (see definition of the poloidal current eq. (8)). In the case of anti-aligned rotator, i.e.  $\mu$  is antiparallel to  $\Omega$ , all signs of the physical quantities related to the charge and current should be reversed.

Calculations have been performed for the following values of  $x_0$ : 0.15; 0.2; 0.3; 0.4; 0.5; 0.6; 0.7; 0.8; 0.9; 0.95; 0.99; 0.992. A unique solution has been found for each of the above  $x_0$ 's. Let us consider in details physical properties of the obtained solutions.

### 4.1 Poloidal current

The poloidal current density  $S$ , calculated from the formula (48), does not deviate for more than  $\sim 20$  per cents from the values given by the Michel's solution (Michel 1973b)

$$S = -\psi \left( 2 - \frac{\psi}{\psi_{\text{last}}} \right), \quad (50)$$

see Fig 4. The smaller  $x_0$ , the smaller this deviation. The structure of the magnetosphere depends strongly on the poloidal current distribution. In solutions with  $x_0 \gtrsim 0.6$  there is a domain in the open field line zone, where *volume* return current flows. However, only a small part of the return current flows there, the main part flows inside the

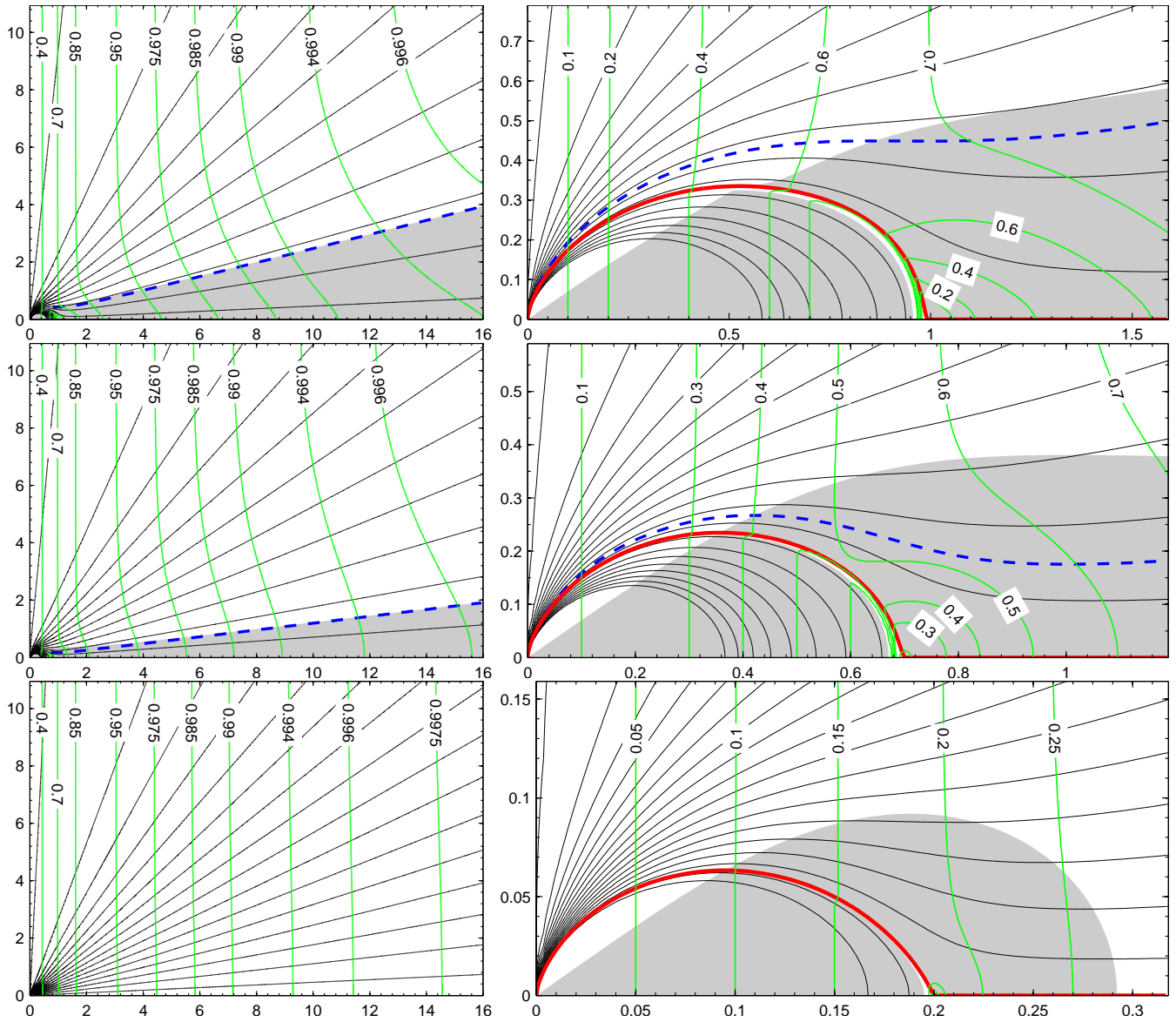


**Figure 3.** Global structure of the magnetosphere for  $x_0 = 0.992$  – top figures,  $x_0 = 0.7$  – middle figures,  $x_0 = 0.2$  – bottom figures. Magnetic flux surfaces are shown by thin solid lines, the labelled vertical lines are contours of the drift velocity, grey area is the domain where the GJ charge density is positive. Dashed line separates regions with direct (above the line) and return (below the line) volume currents. The separatrix is shown by the thick solid line. On the left figures almost the whole calculation domain is shown, on the right figures – the central part of the calculation domain. Distances along  $x$ -axis (horizontal) and  $z$ -axis (vertical) are measured in LC radius  $R_{LC}$ .

current sheet. The size of this domain gets smaller with decreasing of  $x_0$ , and for  $x_0 \lesssim 0.6$  the return current flows only along the separatrix, see Fig. 3. Qualitatively this property of solutions could be explained as the following. At the LC the condition (39) is satisfied, so if  $\partial_x \psi$  changes the sign the same occurs with the current term  $SS'$ , and the poloidal current density changes the sign. Magnetic field lines close to the null point are bend to the equatorial plane, but at large distance they become radial. So, for  $x_0$  close to 1  $\partial_x \psi < 0$  for some field lines, and volume return current must flow along them. When  $x_0$  decreases, more and more magnetic field lines at the LC will be bend away from the equatorial plane until there will be no lines bend to the equator. For field lines

bend from the the equatorial plane  $\partial_x \psi > 0$  and there is no volume return current along them.

A convenient representation of the current density in the closed field line zone could be given by the current density distribution in the polar cap  $j_{pc}$ . In our notations the current density in the polar cap of pulsar normalised to the Goldreich-Julian current density  $j_{GJ} \equiv \rho_{GJ} c$  is given by (see appendix A, eq.(A6))

$$j_{pc} = |j_{GJ}| \frac{1}{2} S' \left( \left( \frac{\theta}{\theta_{pc}} \right)^2 \psi_{last} \right), \quad (51)$$

where  $\theta/\theta_{pc}$  is the colatitude normalised to the colatitude of the polar cap boundary  $\theta_{pc}$ , it is connected to the func-

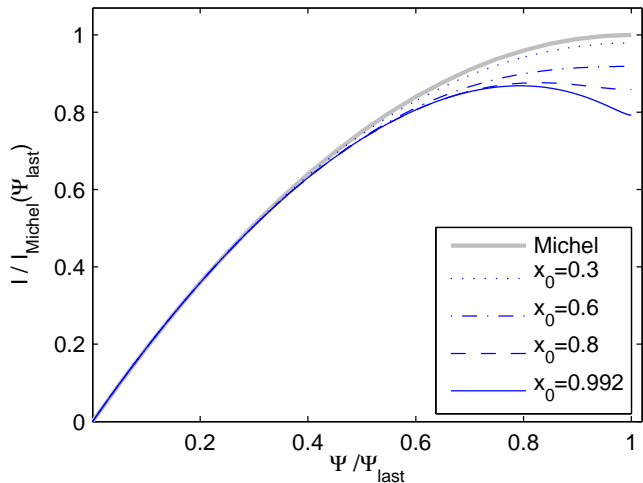


**Figure 4.** Poloidal current distribution in the open field line zone normalised to the poloidal current from the corresponding Michel’s solution. Inside the current sheet, for  $\psi_{\text{last}} \leq \psi \leq \psi_{\text{last}} + d\psi$ , (not shown here) the poloidal current decreases to 0

tion  $\psi$  through the relation  $\theta/\theta_{\text{pc}} = \sqrt{\psi/\psi_{\text{last}}}$ . In Fig. 5  $j_{\text{pc}}$  is shown for several solutions with different  $x_0$ ’s. The current density never exceeds the corresponding GJ current density and goes to zero at the polar cap boundary. The latter property is the consequence of the assumed magnetosphere’s topology. Indeed, from the condition at the LC, eq.(39), the current density along a given magnetic surface is proportional to the partial derivative  $\partial_x \psi$  at the LC, but in configurations with Y null point  $\partial_x \psi = 0$  for  $\psi = \psi_{\text{last}}$ . The deviation of the current density  $j_{\text{pc}}$  from the GJ current density increases close to the polar cap boundaries with increasing of  $x_0$ . For solutions with  $x_0 \gtrsim 0.6$  the current density  $j_{\text{pc}}$  changes the sign at some point near the boundary. On the other hand,  $j_{\text{pc}}$  never exceeds the corresponding Michel current density and approaches  $j_{\text{Michel}}$  when  $x_0$  decreases.

## 4.2 Drift velocity and force-free approximation

The drift velocity in our notations is given by

$$u_{\text{D}} \equiv \frac{|U_{\text{D}}|}{c} = \frac{\Omega \varpi}{c} \frac{B_{\text{pol}}}{B} = \frac{x}{\sqrt{1 + \frac{S^2}{(\partial_x \psi)^2 + (\partial_z \psi)^2}}}, \quad (52)$$

$B_{\text{pol}}$  is the poloidal component of magnetic field. The light surface, i.e. the surface where the force-free approximation breaks down coincide with the surface, where  $u_{\text{D}} = 1$ . We verified the applicability of the force-free approximations in each case. For most of the cases calculations have been performed in the domain with  $x_{\text{max}} = 8, z_{\text{max}} = 7$ , but for  $x_0 = 0.2; 0.7; 0.992$  we performed calculations also with  $x_{\text{max}} = 16, z_{\text{max}} = 14$ . In all cases the light surface is located somewhere outside of these domains, see Fig. 3. The drift velocity distribution for solutions with  $x_0$  close to 1 even at large distances from the null point differs significantly from one in corresponding Michel’s solution (the solution with the same  $\psi_{\text{last}}$ ), where the drift velocity is the function of only  $x$ -coordinate. On the other hand, when  $x_0$  decreases,  $u_{\text{D}}$  approaches the values from the corresponding Michel’s solution.

## 4.3 Charge distribution in the magnetosphere

Goldreich-Julian charge density in the magnetosphere in our notations is given by

$$\rho_{\text{GJ}} = \rho_0 \frac{SS' - \frac{2}{x} \partial_x \psi}{1 - x^2}, \quad \rho_0 \equiv \frac{\mu}{4\pi R_{\text{LC}}^4}. \quad (53)$$

Close to the rotation axis the GJ charge density is negative and with increasing of the colatitude it becomes positive. While for solutions with  $x_0 \gtrsim 0.6$  the domain of positively charged plasma extends to infinity, for solutions with smaller  $x_0$ ’s it becomes finite (cf. plots for  $x_0 = 0.2$  with other plots in Fig. 3). The reason for this is the following. At large distance from the light cylinder magnetic field lines becomes radial, so  $\partial_x \psi$  is always greater than 0. Hence, there only the term  $SS'$  is responsible for changing of the charge density sign. However  $SS'$  for  $x_0 \lesssim 0.6$  never changes the sign, see left plots in Fig. 3. For the same reason the volume return current always flows through the positively charged domain. Close to the NS it passes through the layer where charge density changes the sign, see right plots in Fig. 3. At this layer the so-called outer-gap cascade should develop (see e.g. Cheng et al. 1976; Takata et al. 2004).

The force-free solution fixes not only the volume charge density, but also the charge density of the current sheet. As the electric field at opposite sites of the current sheet is different, the current sheet must have nonzero surface charge density. In Fig. 6 we plotted the linear charge density  $\Sigma$  of the current sheet as a function of distance  $l$  along the separatrix

$$\Sigma \equiv 2\pi \varpi \sigma, \quad (54)$$

where  $\sigma$  is the charge density of the current sheet.  $\Sigma$  represents the total charge of a volume co-moving with particles flowing along the separatrix with the constant speed, emitted at the same time (either at the NS or at “infinity”).  $\Sigma \equiv \text{const}$  would imply a constant velocity flow of particles of *one* sign. However for each solution  $\Sigma$  is non-monotonic function with discontinuity in the null point. Such complicated dependence of  $\Sigma$  on  $l$  implies some non-trivial physics connected with particle creation in the current sheet, which is discussed in the next section.

This complicated dependence of the current sheet charge density is easy to understand if one consider the so-called “matching condition” at the separatrix. As it was shown by Lyubarskii (1990)<sup>4</sup>, at the current sheet the following condition for electric and magnetic field in closed (c) and open (o) field line domains should be satisfied

$$E_c^2 - B_c^2 = E_o^2 - B_o^2. \quad (55)$$

This follows from integration of equation (38) across the current sheet. In the closed field line zone there is no toroidal magnetic field. As it follows from eqs. (14) and (8) the electric field

$$E = x B_{\text{pol}}. \quad (56)$$

Substituting this equation into equation (55) we get

$$B_{\text{pol},c}^2 - B_{\text{pol},o}^2 = \frac{B_{\phi,o}^2}{1 - x^2}. \quad (57)$$

<sup>4</sup> see also Okamoto (1974), eq. (69)

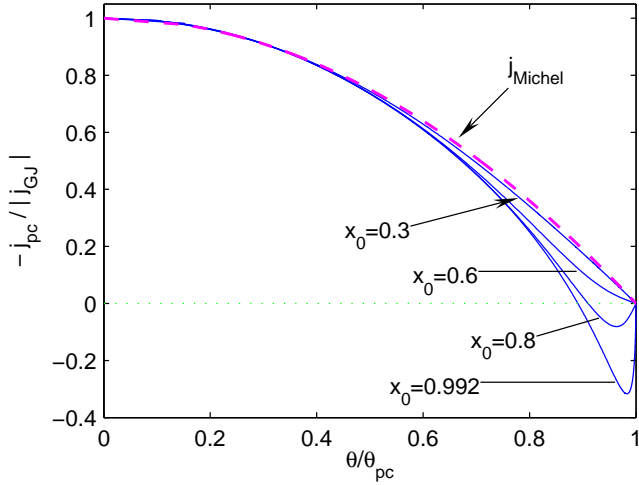


**Figure 5.** Current density distribution in the polar cap of pulsar  $j_{pc}$  as a function of the colatitude.  $j_{pc}$  is normalised to the Goldreich-Julian current density  $|j_{GJ}|$  and the colatitude is measured in units of the polar cap boundary colatitude  $\theta_{pc}$ .

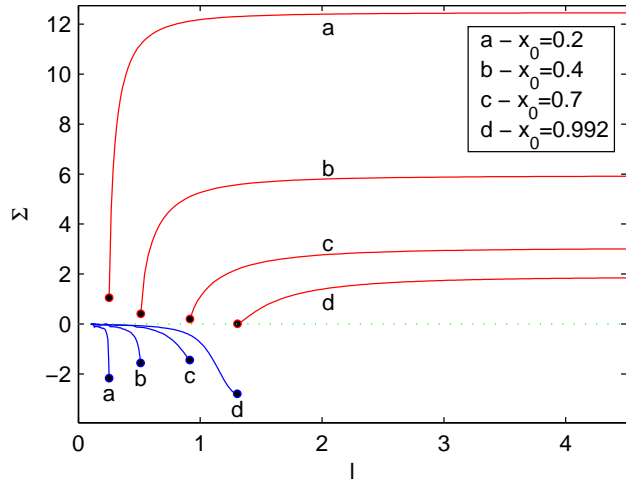


**Figure 6.**  $\Sigma$  – linear charge density of the current sheet (see text) as a function of the distance  $l$  along the current sheet.  $\Sigma$  is normalised to  $0.5\mu/R_{LC}^2$ .  $l$  is measured in units of  $R_{LC}$ . The points mark the position of the corresponding null point. Note the jump in the charge density at these points. The dotted line corresponds to  $\Sigma = 0$ .

From this and equation (56) follows that  $E_c > E_o$  and the charge density in the current sheet between closed and open field line domain,

$$\sigma = \frac{1}{4\pi}(E_o - E_c), \quad (58)$$

is always *negative*. On the other hand, from the symmetry of the system – the electric field in regions 2 and 2' in Fig. 1 has different directions, – the charge density of the current sheet in the open field line zone

$$\sigma = \frac{1}{2\pi}E_o \quad (59)$$

is always *positive*

The total charge of the system, i.e. the charge of the NS, the magnetosphere and the current sheet together must be

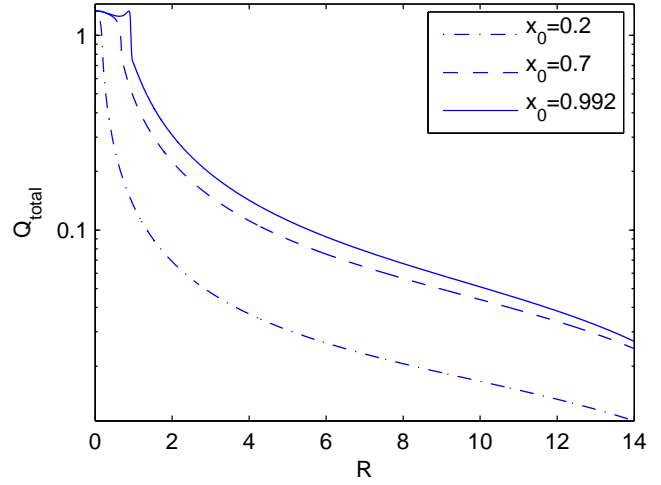


**Figure 7.** The total charge inside the sphere of the radius  $R$  centred at the NS: charge of the NS + charge in the magnetosphere obtained by direct integration of  $\rho_{GJ}$ .  $Q_{total}$  is normalised to  $0.5\mu/R_{LC}$ .  $R$  is measured in units of  $R_{LC}$ .

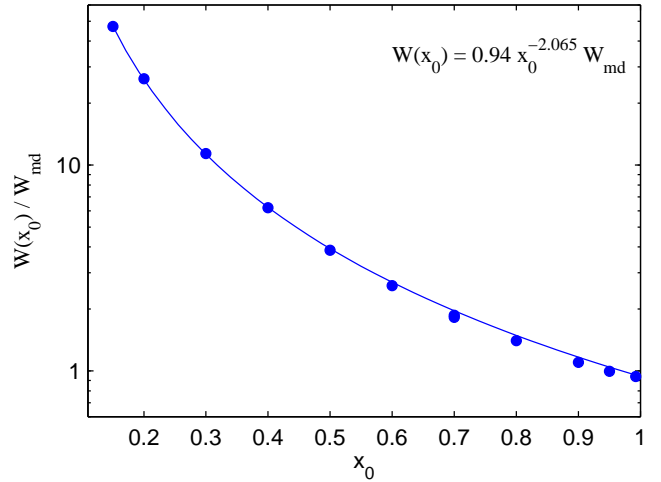


**Figure 8.** Energy losses of the aligned rotator as a function of  $x_0$  in units of the corresponding magnetodipolar energy losses  $|W_{md}|$ .

zero. The boundary condition (45) implies that the total flux of electric field through the sphere of a large radius is zero, hence the total charge of the system must be zero. In Fig. 7 the total charge inside the sphere centred at the coordinate origin is plotted as a function of its radius. The total charge of the system goes rapidly to zero at large distances from the NS. This plot could be also considered as an additional test of the numerical procedure, as the conservation of the total charge is not incorporated into the numerical scheme.

#### 4.4 Energy losses

Energy losses of the aligned rotator in our notations are given by the formula

$$W = |W_{md}| \int_0^{\psi_{last}} S d\psi, \quad (60)$$

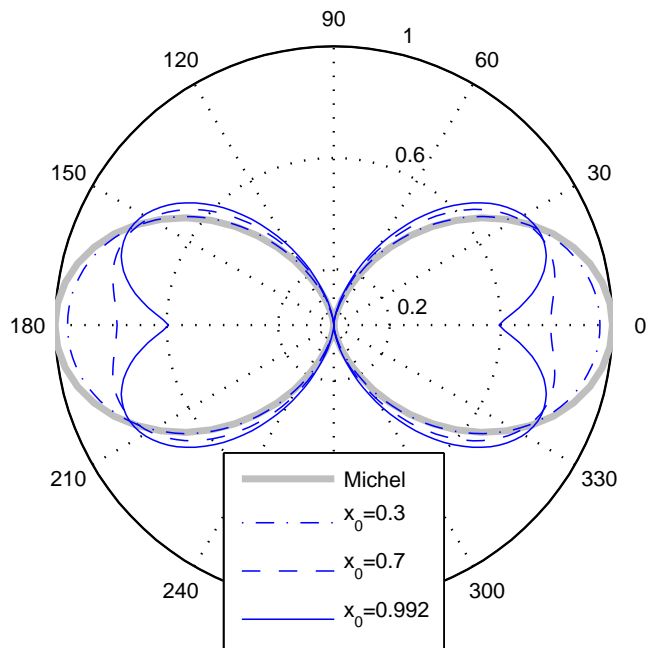


**Figure 9.** Angular distribution of the energy flux  $dW/d\omega$  normalised to  $-\psi_{\text{last}}^2 |W_{\text{md}}|/(4\pi)$ , see eqs. (64) and (65). The distributions shown here are taken at  $R = 4R_{\text{LC}}$  and correspond to their asymptotic forms, see text.

where  $|W_{\text{md}}|$  is the absolute value of magnetodipolar energy losses, here defined as

$$|W_{\text{md}}| = \frac{B_0^2 R_{\text{NS}}^6 \Omega^4}{4c^3}, \quad (61)$$

see appendix B, eqs. (B7), (B5). In the obtained set of solutions  $W$  is function of  $x_0$ . With decreasing of  $x_0$  the amount of open magnetic field lines increases and, as the poloidal current dependence on  $\psi$  does not changes substantially, the energy losses of aligned rotator increases with decreasing of  $x_0$ , see Fig. 8. Obtained dependence of energy losses  $W$  on the position of the null point  $x_0$  could be surprisingly well fitted by a single power law

$$W(x_0) \approx -0.94 x_0^{-2.065} |W_{\text{md}}|. \quad (62)$$

This formula is similar to the one obtained from analytical estimations using Michel current distribution (see appendix B, eq.(B9))

$$W(x_0) \approx -\frac{2}{3} x_0^{-2} |W_{\text{md}}|. \quad (63)$$

The angular distribution of the energy flux (see appendix B, eq. (B4))

$$\frac{dW}{d\omega} = \frac{|W_{\text{md}}|}{4\pi} S \frac{\sqrt{x^2 + z^2}}{x} (z \partial_x \psi - x \partial_z \psi). \quad (64)$$

In Fig. 9 this distribution is shown for several solutions with different  $x_0$ . The Poynting flux distribution quickly reaches its asymptotic form at distance from the null point of the order of  $1 - 2 R_{\text{LC}}$ . For example, in the case of  $x_0 = 0.99$  distributions taken at  $R = 4$  and  $R = 14$  differs by no more than  $\sim 3$  per cents. For configurations with smaller  $x_0$ 's this deviation is even less. The smaller  $x_0$  the closer the angular energy flux distribution to the angular distribution in Michel's solution

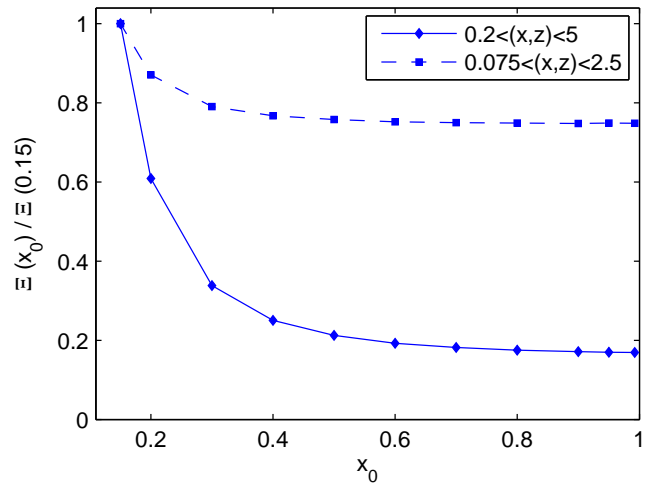


**Figure 10.** Total energy of electromagnetic field in two different volumes of fixed sizes as a function of  $x_0$ .  $\Xi$  is normalised to the corresponding value of  $\Xi(x_0 = 0.15)$ .

$$\frac{dW}{d\omega} = -\frac{|W_{\text{md}}|}{4\pi} \psi_{\text{last}}^2 \sin^2 \theta, \quad (65)$$

because for small  $x_0$  the solution at large distances is very close to the Michel's solution. In spite of recent works on modelling of jet-torus structure seen in Crab and other pulsars (see Komissarov & Lyubarsky 2003; Bogovalov et al. 2005), we note that magnetosphere configurations with larger  $x_0$  would stronger support development of instabilities due to more asymmetric energy deployment into the periphery, providing more pronounced disk structure.

#### 4.5 Total energy of the magnetosphere

The total energy of electric and magnetic fields in the magnetosphere  $\Xi \equiv \int (B^2 + E^2)/(8\pi) dV$  would give information which configuration the system tries to achieve, the configuration with the minimal possible energy. Obviously for the obtained solutions we could calculate the energy only in a finite domain. Another problem is very rapid increase of magnetic field in the central parts, as  $r^{-3}$ . As the magnetic field close to the NS is dipolar for each configuration, we calculate the total energy in a domain excluding the central parts. In order to verify the independence of the result on a particular domain we calculate the total energy in the magnetosphere in two different domains for each solution. These domains are defined as  $0.2 \leq x \leq 5, 0.2 \leq z \leq 5$  and  $0.075 \leq x \leq 2.5, 0.075 \leq z \leq 2.5$ . The results are plotted as a function of  $x_0$  in Fig. 10. The total energy of the magnetosphere increases with decreasing of  $x_0$ , so the magnetosphere will try to achieve the configuration with the maximal possible  $x_0$ .

#### 4.6 Solution with $x_0 \rightarrow 1$

The special case of  $x_0 \rightarrow 1$  has been considered by several authors, because it was believed to be the real configuration of a pulsar magnetosphere (Lyubarskii 1990; Contopoulos et al. 1999; Uzdensky 2003; Gruzinov 2005; Komissarov 2005). This case is peculiar in the sense, that magnetic field in the closed field line zone diverges in the Y

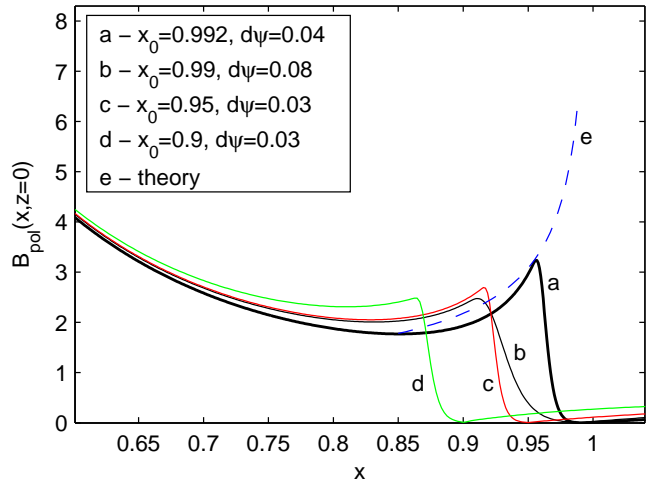


**Figure 11.** Poloidal magnetic field strength in the equatorial plane as the function of  $x$ .  $B_{\text{pol}}$  is normalised to  $\mu/R_{\text{LC}}^3$ . By the dashed line the theoretical prediction for  $B_{\text{pol}}(x, 0)$  is shown for solution with  $x_0 = 0.992$ , eq.(66).

null point. Indeed, from equation (57) it follows that near the null point, when  $x_0 \rightarrow 1$

$$B_{\text{pol}} \approx \frac{\mu}{R_{\text{LC}}^3} \frac{|S|}{\sqrt{2(1-x)}}. \quad (66)$$

While the presence of the singularity was noted by Lyubarskii (1990) and Uzdensky (2003), Gruzinov (2005) firstly realised that such singularity is admitted, as it does not lead to the infinite energy of magnetic field in the region surrounding the null point. In Fig. 11 the strength of the poloidal magnetic field along the  $x$ -axis is plotted for different solutions. By the dashed line the relation (66) is shown. We see that when  $x_0$  approaches the LC the magnetic field inside the closed zone begins to grow close to the null point. This increase is more pronounced when the thickness of the current sheet decreases. Agreement between the curve for  $x_0 = 0.992$ ,  $d\psi = 0.4$  and the dashed line is quite good.

Gruzinov (2005) solved an equation for the separatrix in the vicinity of the null point  $x_0 = 1$  and have found that the angle at which separatrix intersects the equatorial plane should be  $77.3^\circ$ . In our calculations we found this angle to be  $\approx 78^\circ$  for  $x_0 = 0.992$ ,  $d\psi = 0.04$  and  $\approx 70^\circ$  for  $x_0 = 0.99$ ,  $d\psi = 0.08$ . So, our numerical solution shows good agreement with the analytical one. Energy losses found by Gruzinov (2005) are  $1.0 \pm 0.1$ , what quite good agrees with values for  $W$  from Table 1. Value of  $\psi_{\text{last}} = 1.23$  calculated by Contopoulos (2005) coincide with ones from Table 1 and is close to  $\psi_{\text{last}} = 1.27$  obtained by Gruzinov (2005), although both of these results have been obtained with codes having worse numerical resolution than the code used in this work.

## 5 DISCUSSION

It seems naturally to assume, that force-free configurations are energetically preferably in comparison with configurations where there are geometrically large volumes with par-

allel electric field<sup>5</sup>. Accepting this, we conclude that magnetosphere of a pulsar should evolve through a set of force-free configurations. It does not necessary mean that for a relatively short transition time the system could not be essentially non-force-free, but rather that the most time the magnetosphere of an active pulsar is force-free.

### 5.1 Polar cap cascades and force-free magnetosphere

In a force free configuration the current density distribution is not a free parameter, it is set by the structure of the magnetosphere, for example, by the value of  $x_0$  in the case of Y-configuration. However, the current in the magnetosphere of pulsar is supported by electron-positron cascades in the polar cap, i.e. the most of current carriers are produced in the magnetosphere and are not supplied from external sources. Independently of neutron star crust properties, i.e. whether or not charged particles could be extracted from the surface, in polar cap of young pulsars electron-positron cascades are developed filling the magnetosphere of the star with particles (Ruderman & Sutherland 1975; Scharlemann et al. 1978; Muslimov & Tsygan 1992). Also these particles are necessary in order to support MHD like structure of the magnetosphere. The current in the magnetosphere flows trough this cascade region, hence, the cascade, which properties depend on local magnetic field structure, has to adjust to the global properties of the magnetosphere too, namely to the current density flowing through it. We focus here on the case of stationary cascades. The hypothesis about stationarity of the polar cap cascades, when temporal variations of the accelerating electric field over the whole polar cap is much less than the accelerating field itself is widely adopted (e.g. Daugherty & Harding 1982; Ruderman & Sutherland 1975). We briefly address also the case of essentially non-stationary cascade (Levinson et al. 2005).

As it was shown by Lyubarskij (1992), for current adjustment in the stationary cascades a particle inflow from the magnetosphere into the cascade region is required. The typical current density, self-consistently supported by stationary polar cap cascades, is close to  $j_{\text{G.J.}}$ . For current densities, both larger or smaller, than the Goldreich-Julian one, a particle inflow is necessary. The source of inflowing particles needed for current adjustment could be outer gap cascades, operating at the surface where GJ charge density changes the sign (Cheng et al. 1976). On the other hand, inflowing particles could be provided by the pulsar wind, where some outflowing particles could be reversed back to the NS due to momentum redistribution or due to small residual electric field arisen as the magnetosphere tries to support a force-free configuration. However, the zone where particles could flow *toward* the NS is limited by the light cylinder (see Appendix C). So, the source of inflowing particles must be inside the LC.

For Ruderman & Sutherland (1975) cascades, when particles can not be extracted from the NS surface and are produced in the discharge zone, the adjustment mechanism works as follows. Inflow of positrons increases the current

<sup>5</sup> however see e.g. Smith et al. (2001); Pétri et al. (2002)

density, inflow of electrons decreases it. In the first case the inflowing positrons decrease charge density in the Pair Formation Front (PPF) and more electrons is necessary to adjust the charge density to the GJ value. This additional electrons together with inflowing positrons increase the current density. When there is an inflow of electrons, less primary electrons are necessary in order to support the GJ charge density at the PFF. Inflowing electrons are turned back at the PFF, and compensate the inflowing electric current. The outflowing current is only due to the primary electrons from the discharge zone, so the current density is less than  $j_{\text{GJ}}$ .

If particles could almost freely escape from the NS crust, the pulsar operates in the so-called Space Charge Limited Flow (SCLF) regime and the current density can not be essentially less than  $j_{\text{GJ}}$ . Indeed, the charge density in the discharge region, below PFF, is close to  $\rho_{\text{GJ}}$  and accelerating electric field forces charges to outflow with relativistic velocities (Scharlemann et al. 1978; Muslimov & Tsygan 1992). For cascades operating in SCLF regime the mechanism of current adjustment works similarly for inflowing positrons. The particle inflow could *increase* the current density, but not decrease it. Only when the accelerating electric field is almost completely screened, the current density could be significantly less than  $j_{\text{GJ}}$ . However, in order to screen this accelerating field, charged particles inflowing from the magnetosphere must penetrate practically up to the NS surface, i.e. they must have Lorentz factors comparable to the Lorentz factors of particles accelerated in the polar gap. In other words, somewhere in the magnetosphere inside the LC there should be zone(s) where particles are accelerated as effective as they would be accelerated in the polar cap. Either the accelerating field there should be comparable to the one in the polar cap or the size of this zone would be essentially larger than some NS's radii. Both seems to be inappropriate.

In both of these cases in order to support volume *return* current, flowing in the direction opposite to  $j_{\text{GJ}}$ , the accelerated field in the polar cap discharge zone must be completely screened and the particles filling the magnetosphere along magnetic field lines with return volume current must be produced somewhere in the magnetosphere. The accelerating electric field in the polar cap zone, being proportional to the magnetic field strength, is much stronger than any possible accelerating electric field far from the NS. Hence, the presence of the return volume current in the force-free magnetosphere seems to be incompatible with the force-free configurations of the magnetosphere, because the acceleration of particles to the required Lorentz factors with much weaker electric field requires large non-force-free domain(s) in the magnetosphere. The situation with non-stationary cascades is poor investigated, currently there is only one work dedicated to detailed studies of significantly non-stationary cascades – Levinson et al. (2005). However, we see no way how it would be impossible to support both particle production in the polar cap cascade and an average current having opposite direction to the direction of accelerating electric field, see also Arons (1979).

In our consideration we assumed that the GJ charge density in the polar cap does not deviate substantially from its canonical value (Goldreich & Julian 1969)

$$\rho_{\text{GJ}} = -\frac{\Omega B_0}{2\pi c}. \quad (67)$$

This is the case when the boundary of the polar can be considered as equipotential, i.e. having very high conductivity. However if its conductivity is very low and surface charge density distribution at separatrix in the polar cap is different from the one in force-free solution, the GJ charge density can substantially deviate from values given by formula (67). In this case the characteristic current density flowing through the cascade region would be different from the canonical value of  $-(\Omega B_0)/(2\pi)$  and, in principal, it could approach the values required by the global magnetospheric structure, i.e. the problem of current adjustment could be solved by modifying  $\rho_{\text{GJ}}$  instead of adjusting the deviation of  $j$  from  $j_{\text{GJ}}$ . Let us analyse this possibility. The largest part or the whole return current flows along the separatrix. It could be electrons returning from region behind the light surface<sup>6</sup> of ions outflowing from the NS surface (see e.g. Spitkovsky & Arons 2004). If there are electrons in the current sheet close to the NS, then substantial deviation of electric field from the force-free value will give rise to electron-positron cascades producing enough particles to make separatrix near equipotential. Only ions, which much hardly emit photons capable to produce electron-positron pairs could support essentially non-equipotential polar cap boundary. However, as it was mentioned before, each particularly force-free configuration fixes the surface charge density distribution along the current sheet everywhere where it is applicable. Independently on detailed structure of the polar cap zone the surface charge density along the separatrix between closed and open field lines is *negative*, i.e. it must be enough electrons there, or the magnetosphere will be not force-free, see section 4.3 and Fig. 6. Although in the discharge zone above the polar cap force-free approximation is not valid, and arguments of section 4.3 cannot be directly applied to the current sheet at the polar cap boundaries, electrons must be there for the following reason. The current sheet is a region where force-free approximation is broken, at least in some places, for example in the null point, where the surface charge density is discontinuous. As the return current flows in the current sheet, the parallel electric field will be directed from the NS, accelerating electrons in the current sheet toward the NS surface. Hence, in the current sheet at the polar cap boundary there are electrons too and this boundary will be approximately equipotential. Consequently, the GJ charge density in the polar cap should be close to the canonical value (67) and in order to support a force-free configuration of the magnetosphere a current adjustment mechanism is necessary.

For current adjustment high particle density in the magnetosphere is required. Indeed, only a small fraction of all particles could be turned back to the NS. There must be enough inflowing particles for adjusting of the current density in the polar cap, i.e. its number density should be of the order of  $\rho_{\text{GJ}}/e$ . Hence, the particle number density in the magnetosphere must be  $\gg \rho_{\text{GJ}}/e$ . However almost all particles in the magnetosphere are produced in the polar cap and outer gap cascades, and a rather complicated coupling between cascade regions and pulsar magnetosphere arises. The weaker the cascades, the less particles are produced

<sup>6</sup> current sheet is not a force-free domain and considerations from Appendix C are not valid here

there, the smaller deviation from the GJ current density could be supported. Hence, when pulsar becomes older, the number of particles created in polar cap and outer gap cascades is smaller and the maximal deviation of the current density from  $j_{GJ}$  will be smaller. If the magnetosphere remains force-free, its configuration must be changed in order to adjust to the new allowed current density. However, this new configuration would result in different energy losses of the pulsar, i.e. the ratio of the real losses to the losses given by the magnetodipolar formula will be different from the same ratio in previous configuration. So, generally speaking, the evolution of pulsar angular velocity derivative will not follow the power law  $\dot{\Omega} \propto -\Omega^3$ , as it is predicted by the magnetodipolar formula.

In the case of non-stationary cascades there are evidence that no particle inflow into the cascade region may be necessary in order to support current densities both larger and smaller than  $j_{GJ}$  (see Levinson et al. 2005). However, for creation of “wave-like” pattern of accelerating electric field (Levinson et al. 2005), necessary for support of small current densities together with reasonable pair creation rate, high pair density is required. With ageing of the pulsar the maximal achieved electric field and pair density will decrease and shorten the range of allowed current densities. This would lead to the evolution of the magnetosphere similar to the case with stationary cascades.

Arguments presented here are based on qualitative analysis of the polar cap cascade properties. In order to make quantitative predictions a more detailed investigation of polar cap cascades is necessary regarding stationarity, ranges of current densities supported without particle inflow from the magnetosphere, and stability of the cascades in presence of particle inflow from the magnetosphere.

## 5.2 Configurations with Y null point

Let us analyse the behaviour of the magnetosphere of aligned pulsar under assumption that the null point is always of Y type. Here again we mean this in a time average sense, i.e. we neglect possible non-stationary processes (see e.g. Komissarov 2005; Contopoulos 2005) in the current sheet operating on small scales ( $\ll R_{LC}$ ), like building of small plasmoids. If non-stationary variations of the current sheet remains small, the stationary solution should adequately describe the properties of magnetosphere. The total energy of the magnetosphere decreases with increasing of  $x_0$ , see Fig. 10. Apparently the system will try to achieve the configuration with the minimum possible energy, when  $x_0 = 1$ . However, when the restrictions set by the polar cap cascades are taken into account the picture becomes more complicated.

In solutions with Y null point the current density in the magnetosphere close to the polar cap boundaries is always less than the GJ current density, it does not exceed the Michel current density, see section 4.1, Fig. 5. The current adjustment mechanism could adjust the current density to the values *less* than  $j_{GJ}$  for stationary cascade model with no particle escape from the NS surface, in Ruderman & Sutherland (1975) model. If pulsar operates in SCLF regime the current density can not be essentially less than  $j_{GJ}$ . Hence, force-free solutions with Y null point are possible if the stationary polar cap cascade operates

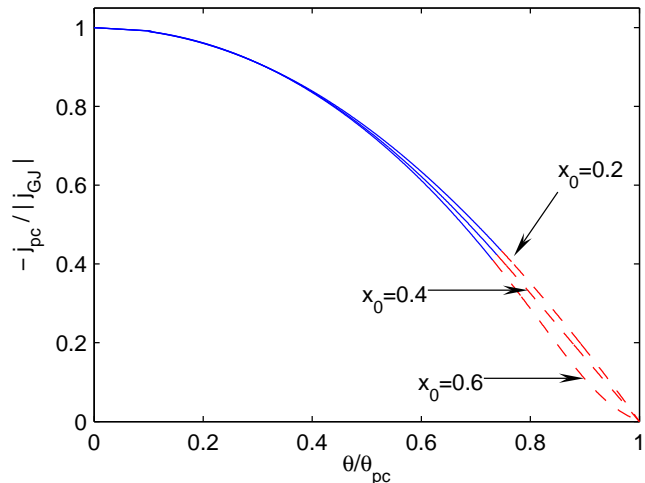


**Figure 12.** Current density distribution in the polar cap of pulsar  $j_{pc}$  as a function of the colatitude. Normalisation of physical quantities is the same as in Fig. 5. The colatitude ranges where the current density deviation from  $j_{GJ}$  could be supported by particles produced in outer gap cascades are indicated by dashed lines. The current density at colatitudes where  $j_{pc}$  is shown by solid line should be supported by particles *reversed* inside the light cylinder.

in Ruderman-Sutherland regime, or if the cascade is significantly non-stationary, the latter case however demands more detailed investigations. On the other hand, for solutions with  $x_0 \gtrsim 0.6$ , the current density  $j_{pc}$  close to the polar cap boundary has different sign than  $j_{GJ}$  and such force-free configurations are probably never realised.

As it was mentioned in section 5.1 the inflowing particles could be produced either in the pulsar wind or in the outer gap cascades. The outer gap cascade could operate at the surface where GJ charge density changes the sign (Cheng et al. 1976). Only relatively small amount of open field lines cross this surface. Hence, particles produced in the outer gap cascades could not adjust the current density along all magnetic field lines. On Fig. 12 we plot current density in the polar cap of pulsar for several  $x_0$  and indicate by the dashed line the colatitudes where particle inflow from the outer gap cascade would be possible. The critical colatitude, where particle inflow from the outer gap cascade is still possible, corresponds to the field line with the smallest  $\psi$  passing the surface of  $\rho_{GJ} = 0$  inside the LC. At other colatitudes reversed particles from the pulsar wind (from inside the LC!) are necessary in order to adjust the current density.

In Fig. 5 one can see that the deviation of the current density from  $j_{GJ}$  although remaining large, becomes smaller with decreasing of  $x_0$ . So, if the magnetosphere remain force-free, with ageing of the pulsar, the configuration should change to the one with smaller current density deviation from  $j_{GJ}$ . Hence, if the force-free magnetosphere preserve its topology, with slow-down of the neutron star the size of the closed field line zone becomes smaller. Immediately consequence of this is the increasing of electromagnetic energy losses respectively to the corresponding “magnetodipolar” energy losses according to equation (62), see Fig. 8. If at some time we approximate the dependence of  $x_0$  on the angular velocity of NS rotation by the power law

$$x_0 \propto \Omega^\xi, \quad (68)$$

where  $\xi$  is in reality a (complicate) function of pulsar age.  $\xi > 0$  because  $x_0$  decreases when pulsar became older. Substituting it into the formula for pulsar energy losses (62) we get

$$W \propto \Omega^\alpha, \quad \alpha = 4 - 2.065 \xi, \quad (69)$$

and for pulsar braking index

$$n = \frac{\ddot{\Omega}}{\dot{\Omega}^2} = \alpha - 1 = 3 - 2.065 \xi, \quad (70)$$

i.e. the braking index is always less than 3!

Let us speculate that configurations with Y null point are energetically preferable over all possible solutions (force-free and non-force-free ones) and the polar cap cascade operates in Ruderman-Sutherland regime. Then as long as particles produced in the cascade regions will be able to support necessary current densities the pulsar magnetosphere should evolve with time as described above, and at each moment of time the configuration should be stable. Indeed, due to reconnection of open field lines in the equatorial current sheet the magnetosphere tries to achieve the energetically most preferably configuration, with  $x_0 = 1$ , but weaker cascades could not inject enough particles into the magnetosphere and support larger deviation of the current density from  $j_{GJ}$ . So,  $x_0$  at each moment of time correspond to the configuration with current distribution having the maximal possible deviation from  $j_{GJ}$ . The polar cap cascade zone is *the part* of the whole system which do not allow closed field zone to have the maximal possible size. Conclusions of Spitkovsky (2005), Komissarov (2005) and McKinney (2006) about instability of all configuration with  $x_0 < 1$  is the result of assumption about possibility of arbitrary current density distribution in the pulsar magnetosphere.

We should note also another peculiarity in Y-configuration – the jump in the surface charge density along the separatrix in the null point, where the charge density changes the sign, see section 4.3 and Fig. 6. The return current flows along the separatrix: electrons to the NS, ions/positrons from the NS. The surface charge density in the current sheet has different sign before and after the null point. We note that there is a jump in the charge density, not just a continuous changing of the charge density like it takes place across the surface where  $\rho_{GJ} = 0$ . What happens in the null point, how such jump in the charge density could be supported when there is a continuous particle flow carrying the return current? Do an electron-positron cascade operates here? Both the magnetic field and soft X-ray radiation of the NS are too weak here and electron-positron pair creation is suppressed. Anyway the problem requires additional investigations.

### 5.3 Alternatives to force-free Y configurations

In the force-free magnetosphere with Y-like null point the deviation of the current density from  $j_{GJ}$  is always large  $\lesssim |j_{GJ} - j_{\text{Michel}}|$ , especially close to the polar cap boundaries. For older pulsar with weak cascades it would be problematic to adjust the current flowing through the polar cap to the required value. On the other hand, even if force-free Y-configurations are energetically more preferably over all

possible solution, the stationary polar cap cascade operating in SCLF regime does not allow current density necessary to support an Y-configuration even in young pulsars. In that cases the magnetosphere could become non-force-free.

The possible alternative to a magnetosphere, becoming non-force-free already at the distance of the order of  $R_{LC}$  from the NS, would be a force-free magnetosphere with X-like null point. The current density deviation from the GJ current density in the magnetosphere with X-like null point would be less that in the Y-configuration for the following reason. In X-configuration with  $x_0 < 1$  condition (39) must be satisfied in points at the light cylinder above  $A$  and below  $A'$ , see Fig. 13. In that points  $\partial_x \psi > 0$ , consequently  $SS'(\psi \leq \psi_{\text{last}}) > 0$  and  $j(\psi \leq \psi_{\text{last}}) < 0$  everywhere, neither changing sign nor approaching zero. In principle, for  $x_0$  not too close to the light cylinder and points  $A, A'$  not too close to the equatorial plane the deviation of the current density from  $j_{GJ}$  could be made rather small allowing even weak cascades to support the current density, because in this case only small correction to the current density would be necessary. It is not clear now do force-free X-configurations exists and how they would look like (this work is in progress), however there is no clear physical reason forbidding such possibility.

For X-configuration the jump in surface charge density of the current sheet in the null point could be avoided or at least reduced in magnitude. Considerations from section 4.3 can be applied to the current sheet separating regions 2(2') and 3 in Fig. 13. If directions of the poloidal magnetic field in these regions coincides<sup>7</sup>, the charge density in this current sheet could be negative too. Indeed, the electric field in regions 2 ( $E_2$ ) and 3 ( $E_3$ ) close to the separatrix in that case has the same direction. If  $E_3 > E_2$ , the charge density of the current sheen is negative and for such configuration the charge density at separatrix does not change the sign, but even if  $E_2 > E_3$  the positive charge density would be less then in the case of equatorial current sheet, when the electric field has to change the sign. If the directions of poloidal magnetic field in these regions are different, the same problem with the current sheet as in Y-configuration arises for any values of the electric field inside the domain 3.

X-configuration was criticised (Lyubarskii 1990) because in the force-free case there is no source of external magnetic field, which could fill the region 3 in Fig. 13. However, ones formed, this region may be supported by the global current system in the magnetosphere. Reconnection in the equatorial current sheet (Komissarov 2005; Contopoulos 2005) could lead to instantaneous formation of magnetic loops, which would grow in size and form some kind of X-configuration. These loops would try to merge with the closed field line zone or fly away, but current distribution in the force-free magnetosphere will not support such configurations, so the resulting X-configuration could be stable. How would force-free solutions with X null point look like is not clear now, may be there could be solutions with many X null points, i.e. when there are several islands

<sup>7</sup> The current sheet in such configuration is necessary, because in the force-free magnetosphere charged particles can not flow across magnetic field lines, so after the null point they should flow along a very thin layer too.

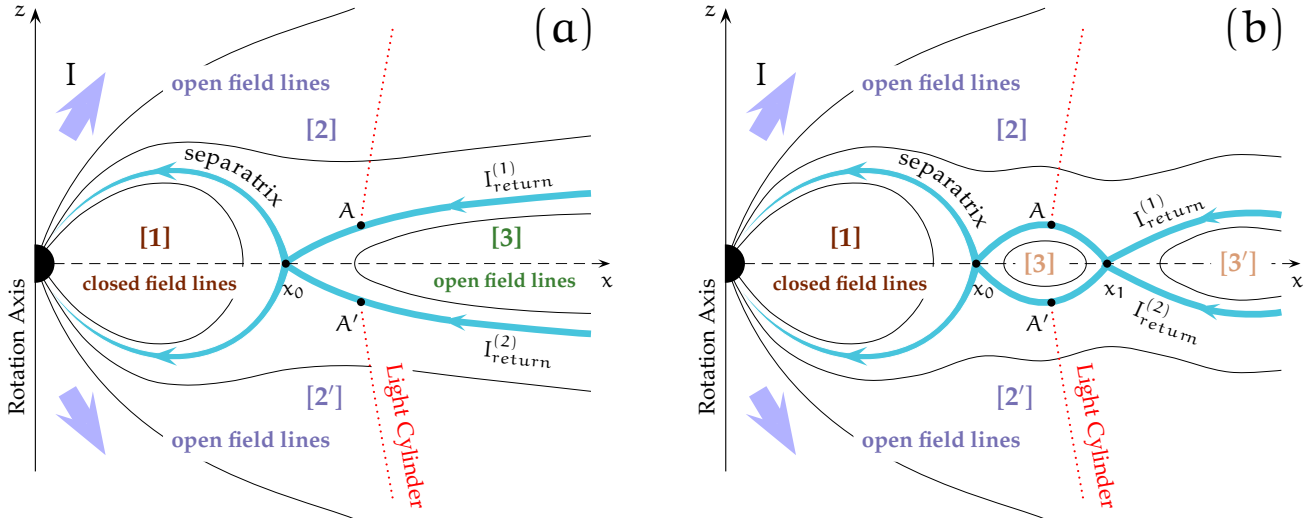


**Figure 13.** Configurations of magnetic field in the magnetosphere of aligned rotator with X-null point. (a) – after the null point  $x_0$  the separatrix goes away from the equatorial plane and never intersects it. There are 3 regions with open magnetic field lines: [2],[2'] and [3]. (b) – after the null point  $x_0$  the separatrix goes away from the equatorial plane but then intersects it (several) times in points  $x_1, \dots$ . There are several regions with closed magnetic field lines: [1],[3] and [3'].

of closed field lines along equatorial plane (see Fig. 13(b)), but such complicated system may be unstable. On the other hand, the configuration shown in Fig. 13(a)<sup>8</sup> can not be entirely force-free. Indeed, there is no poloidal current in zone [3], as it has to have the same direction in both hemispheres, hence, the magnetic field there is purely poloidal. This implies that the plasma here does not rotate and there is no currents in the force-free case which could generate the magnetic field. However, we could speculate that in zone [3] at some (large) distance from the null point, where force-free approximation is broken, a system of currents is build up, which generate the magnetic field also in the force-free domain of zone [3], close to the null point. In this case the magnetosphere may be force-free at several sizes of the LC.

Time-dependent simulations of aligned rotator magnetosphere probably could clear what kind of configuration is realised. Simulations of Spitkovsky (2005); Komissarov (2005) and McKinney (2006) do not incorporate restriction on the electric current in the magnetosphere due to polar cap cascade. In time-dependent codes the restriction set by the polar cap cascades should be formulated in form of boundary conditions on the poloidal current density. This could be done, for example, by introduction of an artificial Ohm's law along open field lines in the “polar cap” of pulsar, i.e. in regions close to the NS surface, like

$$\mathbf{j} = \max(\sigma_{\parallel} \mathbf{E}, \mathbf{j}_{\text{cas}}), \quad (71)$$

where  $\mathbf{j}_{\text{cas}}$  corresponds to the minimal possible current density along the particular field line allowed by cascades.  $\sigma_{\parallel}$  is conductivity along magnetic field lines, specific to each particular code. In order to set these restriction the knowledge of polar cap cascade properties is necessary, what is another very complicated problem.

The possibility of non-stationary magnetosphere also

can not be excluded at the current state of research. In order to decide between possible configurations (e.g. force-free with X or Y null points, non-force-free stationary magnetosphere or significantly non-stationary configurations) more detailed studies of polar cap cascades and stability of the current sheet are necessary.

## 6 CONCLUSIONS

We have studied in details stationary configurations of the force-free magnetosphere of aligned rotator with Y null point. Assumption about Y-configuration of the magnetosphere is very popular and this case had demanded careful investigations. We find a set of force-free solutions parametrised by the position of the neutral point  $x_0$ . Results presented in this work for  $x_0 = 1$  agree very well with ones obtained by other authors (Contopoulos 2005; Gruzinov 2005; Komissarov 2005; Spitkovsky 2005). We calculated physical characteristic of obtained solutions, and analysed properties of force-free magnetosphere with Y-like null point. For solutions with  $x_0$  close to 1, we found that despite similarly distributed magnetic surfaces at large distances from the light cylinder, they differs substantially from the split monopole solution of Michel (1973b) regarding distribution of physical quantities (drift velocity, energy flux distribution, etc.). When the null point lies well inside the light cylinder, solutions approach the Michel one, the agreement being better for smaller values of  $x_0$ 's.

We analysed the role, which cascades in the polar cap play in formation of the overall structure of the magnetosphere. Although its properties depends mostly on the local physics in the polar cap of pulsar, this cascade region sets serious limitation on the current density in the whole magnetosphere. In some sense the non-trivial physics of the cascade plays a role of complicated boundary conditions for MHD equations describing structure of the magnetosphere – arbitrary current density are not allowed. Changes in bound-

<sup>8</sup> such configuration has been considered in several works (e.g. Beskin et al. 1993; Beskin & Malyskin 1998)

ary conditions influence the whole solution. We argue than not all possible Y-configurations can be realised. Moreover, the restrictions set by some cascade models questions the existence of stationary force-free Y-configuration. To our opinion, there are two problems with the force-free magnetosphere in Y-configuration: (i) current density strongly deviates from the GJ current density (ii) the charge density along the current sheet has discontinuity and changes the sign. These problems could be avoided in stationary force-free X-configurations.

We argue that with ageing of pulsar and decreasing of the cascade power, the magnetosphere must involve with time, i.e. it should change to the configurations where the deviation of the current density from  $j_{GJ}$  will be smaller. In the case of force-free Y-configuration the closed field line zone grows slower than the light cylinder during pulsar slow-down. This leads to *decreasing* of pulsar breaking index below the value 3, predicted by the magnetodipolar formula. This effect is present in aligned rotator because of the current adjustment in the polar cap of pulsar. Similar behaviour should be present in configurations with X-like null point too. In analytical model of Beskin & Malyshkin (1998) it was shown that the minimum energy of the magnetosphere is achieved when  $x_0$  approaches the light cylinder. Although their model is an oversimplification of the real problem, this results should be qualitatively true. X-configuration with  $x_0 = 1$  requires strong deviations of  $j$  from  $j_{GJ}$ , so with ageing of pulsar  $x_0$  should decrease, increasing number of the open field lines, leading to increasing of energy losses and decreasing of pulsar breaking index. This should be true also for inclined rotator, at least for not very large inclination angle. Recently Contopoulos & Spitkovsky (2005) proposed another explanation for breaking index of pulsar being less than 3. In their model it is caused also by shrinking of the closed field line zone, but they assumed this is due to differences in characteristic time, at which magnetosphere reaches the new configuration due to reconnection of new magnetic field lines, and the time of increasing of the light cylinder radius. However the reason of such slow reconnection in the current sheet is not clear.

Obtained solutions could be used for comparison with observations. For example, magnetic field lines are differently twisted in different solutions, this could be compared with magnetic field geometry inferred from pulsar polarisation measurements (see Dyks & Harding 2004, and references there). However, the real pulsar magnetosphere could be non-stationary and/or non-force-free, and this issue could be verified only within more detailed time-dependent approach. On the other hand, in the latter case observational manifestations of pulsar will be significantly different from models with force-free magnetosphere, where main emission comes from polar cap and from the outer gap zones.

## ACKNOWLEDGMENTS

I thank V. Beskin for numerous fruitful discussions, helpful suggestions and encouraging comments. I'm grateful to A. Spitkovsky for fruitful discussions and useful comments on the draft version of this article. I acknowledge K. Hirotani, Yu. Lyubarskij, and J. Pétri for discussions. I wish to thank anonymous referee for helpful critical com-

ments. I thank Max-Planck-Institut für Kernphysik (Heidelberg, Germany) for hospitality. This work was partially supported by German Academic Exchange Service (DAAD) grant A/05/05462, and RFBR grant 04-02-16720.

## REFERENCES

- Arons J., 1979, *Space Science Reviews*, 24, 437  
 Beskin V., Gurevich A., Istomin Y., 1993, *Physics of the Pulsar Magnetosphere*. Cambridge University Press  
 Beskin V. S., 2005, "Osesimmetrichnye stacionarnye techeniya v astrofizike" (Axisymmetric stationary flows in astrophysics). Moscow, Fizmatlit, *in russian*  
 Beskin V. S., Gurevich A. V., Istomin I. N., 1983, *Zhurnal Eksperimentalnoi i Teoreticheskoi Fiziki*, 85, 401  
 Beskin V. S., Kuznetsova I. V., Rafikov R. R., 1998, *MNRAS*, 299, 341  
 Beskin V. S., Malyshkin L. M., 1998, *MNRAS*, 298, 847  
 Blandford R. D., 2002, *astro-ph/0202265*  
 Bogovalov S. V., Chechetkin V. M., Koldoba A. V., Ustyugova G. V., 2005, *MNRAS*, 358, 705  
 Cheng A., Ruderman M., Sutherland P., 1976, *ApJ*, 203, 209  
 Contopoulos I., 2005, *A&A*, 442, 579  
 Contopoulos I., Kazanas D., Fendt C., 1999, *ApJ*, 511, 351  
 Contopoulos I., Spitkovsky A., 2005, *astro-ph/0512002*  
 Daugherty J. K., Harding A. K., 1982, *ApJ*, 252, 337  
 Dyks J., Harding A. K., 2004, *ApJ*, 614, 869  
 Goldreich P., Julian W. H., 1969, *ApJ*, 157, 869  
 Goodwin S. P., Mestel J., Mestel L., Wright G. A. E., 2004, *MNRAS*, 349, 213  
 Gruzinov A., 2005, *Phys.Rev.Lett.*, 94, 021101  
 Hibschan J. A., Arons J., 2001, *ApJ*, 554, 624  
 Inghram R. L., 1973, *ApJ*, 186, 625  
 Komissarov S. S., 2002, *MNRAS*, 336, 759  
 Komissarov S. S., 2005, *astro-ph/0510310*  
 Komissarov S. S., Lyubarsky Y. E., 2003, *MNRAS*, 344, L93  
 Levinson A., Melrose D., Judge A., Luo Q., 2005, *ApJ*, 631, 456  
 Lyubarskii Y. E., 1990, *Soviet Astronomy Letters*, 16, 16  
 Lyubarskij Y. E., 1992, *A&A*, 261, 544  
 McKinney J. C., 2006, *astro-ph/0601411*  
 Mestel L., 1973, *Ap&SS*, 24, 289  
 Mestel L., Wang Y.-M., 1979, *MNRAS*, 188, 799  
 Michel F. C., 1973a, *ApJ*, 180, 207  
 Michel F. C., 1973b, *ApJ Letters*, 180, L133  
 Michel F. C., 1991, *Theory of neutron star magnetospheres*. Chicago, IL, University of Chicago Press, 1991, 533 p.  
 Muslimov A. G., Tsygan A. I., 1992, *MNRAS*, 255, 61  
 Okamoto I., 1974, *MNRAS*, 167, 457  
 Pétri J., Heyvaerts J., Bonazzola S., 2002, *A&A*, 384, 414  
 Ruderman M. A., Sutherland P. G., 1975, *ApJ*, 196, 51  
 Scharlemann E. T., Arons J., Fawley W. M., 1978, *ApJ*, 222, 297  
 Scharlemann E. T., Wagoner R. V., 1973, *ApJ*, 182, 951  
 Smith I. A., Michel F. C., Thacker P. D., 2001, *MNRAS*, 322, 209  
 Spitkovsky A., 2004, in Camilo F., Gaensler B. M., eds, *IAU Symposium no.218, "Young Neutron Stars and Their Environments"* *Astronomical Society of the Pacific*, p. 357

- Spitkovsky A., 2005, in T. Bulik B. Rudak G. M., ed., "ASTROPHYSICAL SOURCES OF HIGH ENERGY PARTICLES AND RADIATION" Vol. 801 of AIP Conference Proceedings. p. 253
- Spitkovsky A., Arons J., 2002 Vol. 271 of ASP Conference Series. p. 81
- Spitkovsky A., Arons J., 2004, ApJ, 603, 669
- Sturrock P. A., 1971, ApJ, 164, 529
- Sulkanen M. E., Lovelace R. V. E., 1990, ApJ, 350, 732
- Takata J., Shibata S., Hirokuni K., 2004, MNRAS, 354, 1120
- Timokhin A. N., 2005, astro-ph/0507054
- Trottenberg U., Oosterlee C. W., Schüller A., Brandt A., Oswald P., Stüben K., 2001, Multigrid. Academic Press
- Uzdensky D. A., 2003, ApJ, 598, 446

## APPENDIX A: CURRENT DENSITY IN THE POLAR CAP

The poloidal current density is given by (see Beskin 2005)

$$\mathbf{j}_{\text{pol}} = \frac{\Delta I \times \mathbf{e}_\phi}{\varpi} = \frac{dI}{d\Psi} \mathbf{B}_{\text{pol}}, \quad (\text{A1})$$

the latter expression was obtained by taking into account relation (10). Substituting for  $\mathbf{B}_{\text{pol}}$  the expression for the dipole magnetic field at the NS surface  $\mathbf{B}_{\text{pol}} = B_0(\mathbf{e}_r \cos \theta + (1/2)\mathbf{e}_\theta \sin \theta)$  and expressing  $I$  and  $\Psi$  through normalised quantities we get for the poloidal current density in the polar cap of pulsar

$$j_{\text{pc}} = |j_{\text{GJ}}| \frac{1}{2} S'(\psi) \sqrt{1 - \frac{3}{4} \sin^2 \theta}, \quad (\text{A2})$$

where  $|j_{\text{GJ}}|$  is the absolute value of the Goldreich-Julian current density in the polar cap

$$|j_{\text{GJ}}| = \frac{B_0 \Omega}{2\pi c}. \quad (\text{A3})$$

For dipole magnetic field in the polar cap (see eq. (44))

$$\psi = \frac{R_{\text{LC}}}{R_{\text{NS}}} \sin^2 \theta \approx \frac{R_{\text{LC}}}{R_{\text{NS}}} \theta^2. \quad (\text{A4})$$

The colatitude of the polar cap boundary is  $\theta_{\text{pc}} = 1.45 \times 10^{-2} P^{-1/2} \sqrt{\psi_{\text{last}}}$ ,  $P$  is period of pulsar in seconds. So,  $\theta^2 < \theta_{\text{pc}}^2 \ll 1$  and the term with  $\sin^2 \theta$  in eq.(A2) can be neglected. From equation (A4) we have relation between the colatitude  $\theta$  in the polar cap and the corresponding magnetic flux function  $\psi$

$$\psi = \psi_{\text{last}} \left( \frac{\theta}{\theta_{\text{pc}}} \right)^2. \quad (\text{A5})$$

Substituting this relation into equation (A2) we get

$$j_{\text{pc}} = |j_{\text{GJ}}| \frac{1}{2} S' \left( \left( \frac{\theta}{\theta_{\text{pc}}} \right)^2 \psi_{\text{last}} \right). \quad (\text{A6})$$

## APPENDIX B: ENERGY LOSSES

The poloidal component of Poynting flux in the magnetosphere of aligned rotator is

$$\mathbf{P}_{\text{pol}} = \frac{c}{4\pi} [\mathbf{E} \times \mathbf{B}]_{\text{pol}} = -\frac{\Omega_F \varpi}{c} I \mathbf{B}_{\text{pol}}, \quad (\text{B1})$$

the latter expression was obtained with help of eqs. (8),(14). Expressing  $\mathbf{B}_{\text{pol}}$  through  $\Psi$ , eq. (9), we have for the radial component of the Poynting flux

$$P_r = -\frac{I \Omega_F}{c} \frac{1}{\varpi r} (Z \partial_\varpi \Psi - \varpi \partial_Z \Psi), \quad (\text{B2})$$

where  $r = \sqrt{\varpi^2 + Z^2}$ . Energy losses trough a soling angle  $d\omega$  are  $dW = -r^2 P_r d\omega$ . The angular distribution of energy losses are given by

$$\frac{dW}{d\omega} = \frac{I \Omega_F}{c} \frac{r}{\varpi} (Z \partial_\varpi \Psi - \varpi \partial_Z \Psi). \quad (\text{B3})$$

Using normalised quantities we rewrite this equation as

$$\frac{dW}{d\omega} = \frac{|W_{\text{md}}|}{4\pi} S \frac{\sqrt{x^2 + z^2}}{x} (z \partial_x \psi - x \partial_z \psi), \quad (\text{B4})$$

where  $|W_{\text{md}}|$  is absolute value of magnetodipolar energy losses, here defined as

$$|W_{\text{md}}| \equiv \frac{\mu^2}{R_{\text{LC}}^4} c = \frac{B_0^2 R_{\text{NS}}^6 \Omega^4}{4c^3}. \quad (\text{B5})$$

Energy losses of aligned rotator can be obtained by integration of equation (B3):

$$W = \int_{4\pi} \frac{dW}{d\omega} d\omega = 2 \int_0^{\Psi_{\text{last}}} \frac{2\pi}{c} I \Omega_F d\Psi, \quad (\text{B6})$$

factor 2 appears because energy is carried away by the Poynting flux from both hemispheres. Using normalised quantities introduced at the end of the section 2.1 this formula can be rewritten as

$$W = \frac{\mu^2}{R_{\text{LC}}^4} c \int_0^{\psi_{\text{last}}} S d\psi = |W_{\text{md}}| \int_0^{\psi_{\text{last}}} S d\psi. \quad (\text{B7})$$

Analytical formula for estimation of aligned rotator energy losses could be obtained on the following way. Poloidal current  $S$  for each of obtained solutions does not deviates much from the Michel's current function, eq.(50). Substituting this function into equation (B7) we get

$$W \approx -\frac{2}{3} \psi_{\text{last}}^2 |W_{\text{md}}|. \quad (\text{B8})$$

Dependence of  $\psi_{\text{last}}$  on  $x_0$  we could estimate using magnetic flux function of the dipolar field, eq.(19). Substituting  $\psi^{\text{dip}}(x_0) = x_0^{-1}$  into equation (B8) we get

$$W \approx -\frac{2}{3} x_0^{-2} |W_{\text{md}}|. \quad (\text{B9})$$

## APPENDIX C: THE SIZE OF THE REGION WHERE PARTICLE INFLOW IS POSSIBLE

Charged particles in crossed electric and magnetic fields drift with the velocity  $\mathbf{U}_D$  given by eq. (16), which can be rewritten as

$$\mathbf{U}_D = \frac{\Omega_F \varpi}{B^2} (B_{\text{pol}}^2 \mathbf{e}_\phi - B_\phi \mathbf{B}_{\text{pol}}). \quad (\text{C1})$$

In general, charged particle in the magnetosphere could have two velocity components: one perpendicular to the magnetic field line (the drift velocity) and an additional component along magnetic field line  $U_{\parallel}$ , see Fig. C1. With increasing of the distance from the NS  $U_D$  increases, see Fig. 3. The velocity of the particle  $U$  can not exceed the speed of light,

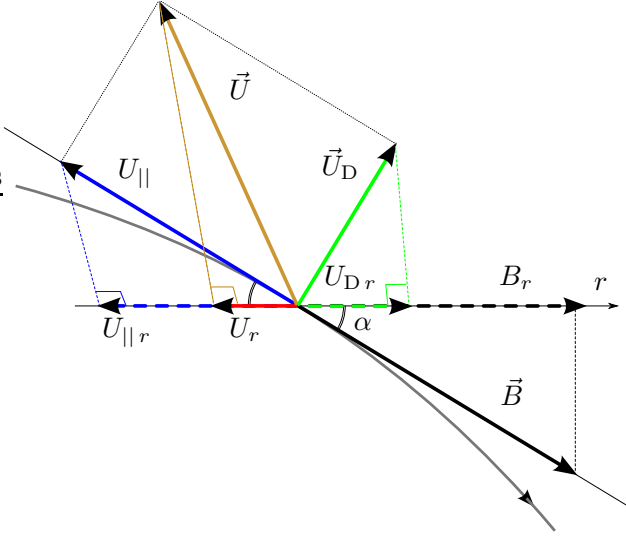


**Figure C1.** Particle velocity decomposition in  $U_{\parallel}$  and  $U_D$ . Magnetic field line is shown by the thick curved line.

hence, the parallel component of particle velocity far from NS must be also smaller. Magnetic field lines far from NS are strongly twisted and at some distance the particle radial velocity component will be positive, i.e. directed from the NS, for any direction of the parallel component. At these distances particles can flow only *from* the NS. Let us show that the size of the domain, where particles could flow to the NS, corresponds to the size of the light cylinder.

From Fig. C1 it is evident that the radial component of the total particle velocity is

$$U_r = U_{D r} + U_{\parallel r}. \quad (\text{C2})$$

The maximal value of the velocity component parallel to the magnetic field is

$$U_{\parallel}^{\max} \simeq \sqrt{c^2 - U_D^2}. \quad (\text{C3})$$

If the radial component of the magnetic field  $B_r > 0$  then for the azimuthal component of magnetic field  $B_{\phi} = -|B_{\phi}|$ . For radial components of particle velocities we have

$$U_{\parallel r}^{\max} = -\frac{B_r}{B} U_{\parallel}^{\max} \simeq -\frac{B_r}{B} c \sqrt{1 - \left(\frac{\Omega_F \varpi}{c}\right)^2 \frac{B_{\text{pol}}^2}{B^2}} \quad (\text{C4})$$

$$U_{D r} = \frac{\Omega_F \varpi}{B^2} |B_{\phi}| B_r \quad (\text{C5})$$

From this the maximal possible velocity component in radial direction is

$$U_r^{\max} \simeq -\frac{B_r}{B} c \left( \sqrt{1 - \left(\frac{\Omega_F \varpi}{c}\right)^2 \frac{B_{\text{pol}}^2}{B^2}} - \frac{\Omega_F \varpi |B_{\phi}|}{c B} \right) \quad (\text{C6})$$

Particles could flow to the NS only if  $U_r^{\max} < 0$ , and this is possible if

$$\sqrt{1 - \left(\frac{\Omega_F \varpi}{c}\right)^2 \frac{B_{\text{pol}}^2}{B^2}} > \frac{\Omega_F \varpi |B_{\phi}|}{c B} \quad (\text{C7})$$

or

$$\varpi < \frac{c}{\Omega_F}, \quad (\text{C8})$$

i.e. only inside the light cylinder. For  $B_r < 0$  we get the same result. The same restriction, namely that particles could

cross the alfvénic surface (light cylinder in our case) only in one direction, is proved to be valid in full MHD case too (see e.g. Beskin 2005).